A new numerical scheme for constrained total variation flows and its convergence

Yoshikazu Giga* Koya Sakakibara† Kazutoshi Taguchi‡ Masaaki Uesaka§

March 22, 2019

Abstract

In this paper, we propose a new numerical scheme for a spatially discrete model of constrained total variation flows, which are total variation flows whose values are constrained in a Riemannian manifold. The difficulty of this problem is that the underlying function space is not convex and it is hard to calculate the minimizer of the functional with the manifold constraint. We overcome this difficulty by "localization technique" using the exponential map and prove the finite-time error estimate in general situation. Finally, we show a few numerical results for the cases that the target manifolds are S^2 and $SO(3)$.

1. Introduction

In this paper, we consider a constrained total variation flow equation (constrained TV flow equation for short):

$$(\mathrm{TVF};u_0)\begin{cases} \dfrac{\partial u}{\partial t} = -\pi_u\left(-\nabla\cdot\left(\dfrac{\nabla u}{|\nabla u|}\right)\right) & \text{in} \quad \Omega\times(0,T), \\ \left(\dfrac{\nabla u}{|\nabla u|}\right)\cdot\nu^{\Omega} = 0 & \text{in} \quad \partial\Omega\times(0,T), \\ u|_{t=0} = u_0 & \text{on} \quad \Omega, \end{cases} \tag{1.1}$$

where $\Omega\subset\mathbb{R}^k\,(k\geq 1)$ is a bounded domain with a Lipschitz boundary $\partial\Omega$, M a C^2-manifold embedded into $\mathbb{R}^\ell\,(\ell\geq 1)$, $u\colon\Omega\times[0,T)\to M$ an unknown, $u_0:\Omega\to M$ an initial datum, π_p an orthogonal projection from the tangent space $T_p\mathbb{R}^\ell(=\mathbb{R}^\ell)$ to the tangent space $T_pM(\subset\mathbb{R}^\ell)$ at $p\in M$, ν^Ω the outer normal vector of $\partial\Omega$ and $T>0$. If π_u is absent, $(\mathrm{TVF};u_0)$ is a standard vectorial total variation flow regarded as the L^2-gradient flow of an isotropic total variation of vector-valued maps:

$$\boldsymbol{TV}(u) := \int_\Omega |\nabla u|_{\mathbb{R}^{k\times\ell}}\,\mathrm{d}x,$$

where $|\cdot|_{\mathbb{R}^{k\times\ell}}$ denotes the Euclidean norm of $\mathbb{R}^{k\times\ell}$. The introduction of π_u means that we impose the restriction on gradient of total variation so that u always takes the values into M. We also call it "M-valued total variation flow" or "1-harmonic map flow"

*Graduate School of Mathematical Sciences, The University of Tokyo. mail:labgiga@ms.u-tokyo.ac.jp

†Graduate School of Science, Kyoto University; RIKEN Interdisciplinary Theoretical and Mathematical Sciences Program (iTHEMS). mail:ksakaki@math.kyoto-u.ac.jp

‡Graduate School of Mathematical Sciences, The University of Tokyo. mail:ktaguchi@ms.u-tokyo.ac.jp

§Research Institute for Electronic Science, Hokkaido University. mail:muesaka@es.hokudai.ac.jp

1.1. Applications in science and engineering

The constrained total variation flows have applications in several fields. First applications of the flow of this type appears in [33], where the authors consider the case that the target manifold M is a two-dimensional sphere S^2, for color image denoising with preserving the brightness. As for the case that the target manifold M is the space of all three-dimensional rotations $SO(3)$, this system is an important prototype of the continuum model for a time-evolution of grain boundaries in a crystal, proposed in [23, 22]. As for the case that the target manifold M is the space of all symmetric positive definite three-dimensional matrices $SPD(3)$, such equations are proposed for denoising diffusion tensor MRI ([4, 28, 9, 35]).

1.2. Mathematical analysis

In spite of its applicability, the mathematical analysis to the manifold-constrained total variation flows is still developing. Two difficulties lie in the mathematical analysis: One is the singularity of the system where ∇u vanishes; second is the constraint with values of flows into a manifold. On the first difficulty, many studies can be found to overcome it. In order to explain the second difficulty, we split notion of solutions into "regular solution" and "irregular solution".

We mean by "regular solution" a solution without jumps. In [18], the existence of a local-in-time regular solution was proved when Ω is k-torus T^k, a manifold M is an $(\ell-1)$-sphere $S^{\ell-1}$ and an initial datum u_0 is sufficiently smooth and of small total variation. Recently, this work has been improved significantly in [15]. In particular, the assumption has been weakened in the case that the domain Ω is convex and the initial datum u_0 is Lipschitz continuous. Moreover, in [15], the existence of global-in-time regular solution and its uniqueness have been proved when the target manifold M has non-positive curvature and initial data u_0 is small.

In [17], it has been proved that rotationally symmetric solutions may break down, that is, lose its smoothness in finite time when Ω is the two-dimensional unit disk and $M = S^2$. Subsequently, in [27], the optimal blowup criterion for initial datum given in [17] was found and it was proved that so-called reverse bubbling blowup may happen.

For "irregular solution", a solution which may have jumps, two notion of solutions are proposed; it depends on the choice of the distance to measure jumps of the function. These choices deduce the different notions of a solution of constrained gradient system, which may not coincide each other.

Weak solutions derived from "extrinsic distance" or "ambient distance", the distance of the Euclidean space in which the manifold M is embedded, is studied in [16, 20]. According to [16], in a space of piecewise constant functions, the existence and the uniqueness of global-in-time weak solution have been established when M is compact, the domain Ω is an interval with finite length, and the initial datum u_0 is piecewise constant. Moreover, in [16], finite stopping phenomena of S^1-valued total variation flows was also proved. On the contrary, for S^2-valued total variation flows, an example that does not stop in finite time was constructed in [20], which will be reproduced numerically by our new numerical scheme and used for its numerical verification in this paper.

Weak solutions derived from "intrinsic distance", the geodesic distance of the target manifold M, was studied in [13, 14, 5]. In [13], the existence and the uniqueness of global-in-time weak solution have been proved when Ω is a bounded domain with Lipschitz boundary, $M = S^1$, and the initial datum u_0 has finite total variation and does not have jumps greater than π. This arguments and results were extended in [5] when the target manifold M is a planer curves. As for the higher dimensional target manifold, the existence of global-in-time weak solution was proved in [14] when the target manifold M is a hyperoctant $S^{\ell-1}_+$ of $(\ell-1)$-sphere.

1.3. Numerical analysis and computation

Constrained discrete total variation flows, which mean spatially discrete models of constrained total variation flows, have been studied in [34, 16, 19, 3, 11, 32].

In [34], discrete models of S^1-valued TV flows and S^2-valued TV flows based on the finite difference method were studied. More precisely, their numerical scheme were proposed and numerical computations were performed by them.

In [3, 11], $S^{\ell-1}$-valued regularized TV flows based on the finite element methods were studied. In their works, the existence and the uniqueness of global-in-time solution of the discrete models were established and numerical computations were performed. We remark that convergence of the discrete model to the original model was also studied. However, its argument has some flaws which were pointed in [13]. In these works, the Ginzburg–Landau type penalization term is introduced for expressing the manifold constraint and the total variation term is relaxed.

In [16, 18, 19, 32], discrete models of constrained TV flows based on finite element method with piecewise constant functions were studied. These discrete models itself are important models of denoising of manifold-valued digital images. In case of one-dimensional spatial domain, solutions of the discrete models coincide with irregular solutions of the corresponding original model derived by ambient distance but not in the case of higher dimensional domain. In one-dimensional spatial domain, the existence and the uniqueness of global-in-time solution to the discrete models were established in [16]. Moreover, numerical computations of S^1-valued discrete models were performed. These discrete models are formulated as ordinary differential inclusions which means differential equation with multi-valued velocity. There are two key ideas in [16] to solve them. First one is computation of the canonical restriction of the multi-valued velocity. Second one is to use facet-preserving phenomenon of flows. We also emphasize that these two key ideas do not work in higher dimension rather than one. In such case, the existence and the uniqueness of global-in-time solution of the discrete model were established in [18, 19, 32]. Numerical computations of these discrete models, however, were not performed.

1.4. Contribution of this paper

This paper is dedicated to study of a numerical scheme for simulation of a discrete model, which is studied in [18, 19, 32], of constrained TV flow based on the finite element method with piecewise constant functions. In particular, we propose a new numerical scheme, and study its theoretical properties. We also perform numerical simulations based on the proposed scheme. We overview main three contributions below:

1.4.1. New numerical scheme

A constrained discrete TV flow is formulated as a gradient flow in a suitable manifold. Hence, one can use the minimizing movement scheme (see [2]) to simulate it. It is summarized as follows:

Let $H := (H, \langle\cdot,\cdot\rangle_H)$ be a real Hilbert space, E be a submanifold of H, $\mathcal{F}$ be an extended real-valued functional on H. Let $I := [0, T)$ be a time interval and $\boldsymbol{\tau} := \{\tau^{(n)}\}_{n=0}^{N}$ be a time partition of I, that is, $\boldsymbol{\tau}$ satisfies

$$0 =: \tau^{(0)} < \tau^{(1)} < \ldots < \tau^{(N-1)} < \tau^{(N)} = T.$$

Let $|\boldsymbol{\tau}| := \sup\{\tau^{(n)} - \tau^{(n-1)} \mid n = 1, \ldots, N\}$ denote the maximal width of $\boldsymbol{\tau}$. Then, a sequence $\left\{u_{\boldsymbol{\tau}}^{(n)}\right\}_{n=0}^{N}$ in E generated by a minimizing movement scheme (MMS; $\boldsymbol{\tau}, u_0$) of $\mathcal{F}$ is defined by

the following procedure:

Algorithm 1 ((MMS; $\boldsymbol{\tau}, u_0$): Minimizing Movement Scheme)**.**

1. *If* $n = 0$*, then set* $u_{\boldsymbol{\tau}}^{(0)} := u_0$*.*
2. *If* $n \geq 1$*, then* $u_{\boldsymbol{\tau}}^{(n)}$ *is defined as a minimizer of the optimization problem* $(\mathrm{OP}; \tau^{(n)} - \tau^{(n-1)}, u_{\boldsymbol{\tau}}^{(n-1)})$*:*

$$\textit{Minimize } \Phi(u; \tau^{(n)} - \tau^{(n-1)}, u_{\boldsymbol{\tau}}^{(n-1)}) \textit{ subject to } u \in E,$$

where

$$\Phi(u; \tau, v) := \tau \mathcal{F}(u) + \frac{1}{2} \|u - v\|_H^2, \quad u, v \in E, \quad \tau > 0.$$

In the viewpoint of numerical computation, it is not easy to solve the optimization problems in the scheme since the optimization problems are classified as Riemannian optimization problems which are an optimization problems with Riemanninan manifold constraint. Theory of *smooth* Riemannian optimization, that is, Riemannian optimization problem whose object function is smooth, is well-studied, and we refer to [1] for its systematical presentation. On the other hand, theory of *non-smooth* Riemannian optimization is still scarcely explored as a subfield of theory of Riemannian optimization. Here, we point out that the optimization problems derived by minimizing movement scheme of constrained discrete total variation flows are non-smooth Riemannian optimization problems. We refer to [24, 36, 8, 37] as its references. Moreover, theory of non-smooth Riemannian optimization is generalized to theory of non-smooth and non-convex optimization with separable structure in [25]. Although there are several studies in this way, it is under development as compared with the linearly constrained problem. Therefore, in this paper, we propose a numerical scheme $(\mathrm{MMS}^\dagger; \boldsymbol{\tau}, u_0)$ of $\mathcal{F}$ each of whose step includes a *linearly constrained* optimization problem instead of the Riemanninan constraint problem $(\mathrm{OP}; \tau^{(n)} - \tau^{(n-1)}, u_{\boldsymbol{\tau}}^{(n-1)})$. That is as follows:

Algorithm 2 ((MMS†; $\boldsymbol{\tau}, u_0$): Proposed Scheme)**.**

1. *If* $n = 0$*, then set* $u_{\boldsymbol{\tau}}^{(0)} := u_0$*.*
2. *If* $n \geq 1$*, then* $u_{\boldsymbol{\tau}}^{(n)} \in E$ *is defined as follows:*
   (a) *Take* $X_{\boldsymbol{\tau}}^{(n-1)}$ *as a minimizer of the optimization problem* $(\mathrm{OP}^\dagger; \tau^{(n)} - \tau^{(n-1)}, u_{\boldsymbol{\tau}}^{(n-1)})$*:*

$$\textit{Minimize } \Phi^\dagger(X; \tau^{(n)} - \tau^{(n-1)}, u_{\boldsymbol{\tau}}^{(n-1)}) \textit{ subject to } X \in T_{u_{\boldsymbol{\tau}}^{(n-1)}} E,$$

   where $T_u E (\subset H)$ *denotes the tangent space of* E *at* u *and*

$$\Phi^\dagger(X; \tau, v) := \tau \mathcal{F}(v + X) + \frac{1}{2} \|X\|_H^2, \quad X \in H, \ v \in E, \ \tau > 0.$$

   (b) *Set* $u_{\boldsymbol{\tau}}^{(n)} = \mathrm{Exp}_{u_{\boldsymbol{\tau}}^{(n-1)}}(X_{\boldsymbol{\tau}}^{(n-1)})$ *by using "exponential map"* Exp *in* E*.*

In fact, each problem $(\mathrm{OP}^\dagger; \tau^{(n)} - \tau^{(n-1)}, u_{\boldsymbol{\tau}}^{(n-1)})$ is linearly constrained optimization problem since $T_{u_{\boldsymbol{\tau}}^{(n-1)}} E$ is a linear space. Moreover, each $(\mathrm{OP}^\dagger; \tau^{(n)} - \tau^{(n-1)}, u_{\boldsymbol{\tau}}^{(n-1)})$ is convex if Φ is convex. We remark that the idea using the exponential map appears in the optimization problem in matrix manifolds and in numerical computation of regularizing flows like constrained heat flows (see [1, 6, 7]).

1.4.2. Theoretical properties

In this paper, we study the scheme in two points. Those are "energy decay" and "error rate" for the proposed scheme.

Energy decay is one of the fundamental properties for gradient flows. Hence, it is desirable that a numerical scheme of gradient flows also inherits the energy decay inequality. In this paper, we show that the proposed scheme satisfies the energy decay inequality if the maximal time-width $|\boldsymbol{\tau}|$ is sufficient small.

Error rates are important inequalities that indicate that the scheme can properly approximate the original problem. In this paper, we will establish an error rate between a sequence generated by the proposed scheme and the original constrained discrete TV flow. Since the proposed scheme is a scheme derived from minimizing movement schemes, it can be expected that the proposed scheme has a similar error rate of minimizing movement schemes. The result of error analysis for the minimizing movement scheme appears in [2, 10, 30]. In the classical work [10] of the error analysis in Banach space, $O(\sqrt{|\boldsymbol{\tau}|})$-error estimate was obtained and it is improved to $O(|\boldsymbol{\tau}|)$-error one in [30]. The similar estimate to [10] in a general metric space is shown in [2]. Since our scheme contains the "localization" process, we cannot apply these previous works directly. This estimate, which will be stated in Section 3.3, states that the error of the Rothe interpolation is $O(\sqrt{|\boldsymbol{\tau}|})$. This estimate corresponds to those in [2, 10]. In this paper, we establish $O(\sqrt{|\boldsymbol{\tau}|})$-error estimate for the proposed scheme, which is corresponds to those in [2, 10]. We point out that convergence of an appropriate time-interpolation of numerical solutions to the original flow is obtained from a simple consequence of such an error estimate.

1.4.3. Numerical simulations

The proposed scheme is not enough to simulate constrained discrete TV flow since we need to solve $(\mathrm{OP}^{\dagger}; \tau^{(n)} - \tau^{(n-1)}, u_{\boldsymbol{\tau}}^{(n-1)})$ at each step. We overcome this situation by rewriting $(\mathrm{OP}^{\dagger}; \tau^{(n)} - \tau^{(n-1)}, u_{\boldsymbol{\tau}}^{(n-1)})$ as an iteration, and adopt alternating split Bregman iteration, proposed by [21] , which is effective to the optimization problem with total variation. We refer to [26, 29] for examples of application of this iteration to calculate the crystalline mean curvature flow numerically. One can find a proof of convergence of this iteration in [31].

In this paper, we numerically reproduce the three properties of constrained TV flows. First one is non-finite stopping phenomenon of S^2-valued TV flow which is constructed in [20]. Second one is an error rate of the proposed scheme which is established in this paper. Actually, the example in [20] can be rewritten as a very simple ordinary differential equation, and we can use explicit scheme to simulate it. Therefore, we simulate this example by two methods and compare them to confirm that the error rate is reproduced. Third one is numerical observation that a facet is preserving in most of evolution. In fact, we simulate S^2-valued TV flows with one spatial dimension, which is constructed in [20] and $SO(3)$-valued TV flows with two spatial dimension.

1.4.4. Advantages

The proposed scheme has five advantages:

First, this scheme does not restrict the target manifold M. In many previous studies, the target manifold M is fixed in advance, to sphere for example. Our method, however, can be applied for any Riemannian manifold as target manifold M.

Second, this scheme does not restrict gradient flows. In this paper, we discuss the Neumann problem of constrained TV flow equation only. However, the proposed scheme can be executed

if the linearly constrained problem can be solved at each step. Hence, we can apply the proposed scheme to other constrained gradient flows such as the Dirichlet problem of constrained TV flow equations and the Dirichlet (Neumann) problem of harmonic map flow equations.

Third, the proposed scheme can describe facet-preserving phenomena of constrained total variation flows. In the numerical calculation of the total variation flow, we should pay attention to whether a numerical scheme can adequately simulate the evolution of facet of numerical solutions. Many schemes that have been proposed so far do not generally describe this phenomenon, since the energies are smoothly regularized. However, the proposed scheme can properly describe this phenomenon since the energies in the proposed scheme are convexly modified, not smoothly regularized.

Fourth, the proposed scheme is numerically practical. Especially, if the exponential map and the orthogonal projection π of the target manifold M can be calculated easily, the practical advantage of our scheme is clear. In fact, if M is in class of orthogonal Stiefel manifolds, its orthogonal projection π and its exponential map can be written explicitly. See also [1]. In addition, as mentioned above, our method does not use the projection into the target manifold which is sometimes hard to calculate.

Finally, the proposed scheme is well-defined and we shall prove its error rate as well as its convergence.

1.5. Organization of this paper

The plan of this paper is as follows:

In Section 2, we recall notions and notations for describing constrained discrete TV flows we study in this paper. More precisely, we recall notion of manifolds and define finite element spaces consisting of piecewise constant functions, discrete total variation, and a discrete model of constrained TV flows based on the finite element method with piecewise constant functions.

In Section 3, we propose a new numerical scheme and its theoretical properties "energy decay" and "error rate". In Section 3.1, we explain a new numerical scheme for constrained discrete TV flows and its derivation. More precisely, we derive the proposed scheme starting from the minimizing movement scheme for constrained discrete total variation flows. In Section 3.2, we state that the proposed scheme has energy decay if the maximal time-width is sufficiently small. In Section 3.3, we state that error rate between a sequence generated by the proposed scheme and a constrained discrete TV flow. We see that this error rate implies that the proposed scheme converges to constrained discrete total variation flows if the maximal time-width tends to zero.

In Section 4, we prove the theoretical properties of the proposed scheme described in Section 3. In Section 4.1, we explain the Rothe interpolations and its properties. This interpolation is useful to prove energy decay and convergence rate of the proposed scheme. In Section 4.1.1, we prove an energy decay for the proposed scheme inequality. In Section 4.1.2, we establish an error rate of the proposed scheme. The key of its proof is to establish the evolution variational inequalities, used in [2], of the Rothe interpolation of a sequence generated by the proposed scheme and a solution of constrained discrete TV flow equation.

In Section 5, we perform the results of the numerical experiments by the proposed scheme. More precisely, we rewrite the scheme into a practical version with alternating split Bregman iteration, and we use it to simulate S^2-valued and $SO(3)$-valued discrete total variation flows, respectively.

In Appendix A, we explain the constant C_M which appear in the inequality (2.2) in Section 2 is bounded by explicit quantities in submanifolds in Euclidean space.

Acknowledgement

We are grateful to Professor Takeshi Ohtsuka (Gumma University) for several discussions and comments. Especially, he suggested to us that the alternating split Bregman iteration is suitable for the numerical experiments. This work was supported by KAKENHI No. 26220702 (YG), No. 18K13455 (KS) and the Program for Leading Graduate Schools, MEXT, Japan (KT).

2. Preliminaries

Here and henceforth, we fix the bounded domain Ω in $\mathbb{R}^k$ with a Lipschitz boundary $\partial\Omega$. In this section, we recall notion of submanifolds in Euchlidean space, finite element spaces, and constrained discrete total variation flows.

2.1. Notion and notations of submanifolds in Euclidean space

Let M be a C^2-submanifold in $\mathbb{R}^\ell (\ell \geq 2)$. For $p \in M$, we denote by T_pM and $T_p^\perp M$ the tangent and the normal spaces of M at p, respectively, and write π_p and $\pi_p^\perp$ for the the orthogonal projections from $\mathbb{R}^\ell$ to T_pM and $T_p^\perp M$, respectively. We denote by $\mathrm{II}_p : T_pM \times T_pM \to T_p^\perp M$ the second fundamental form at p in M. Moreover, we define the diameter $\mathrm{Diam}(M)$ and the curvature $\mathrm{Curv}(M)$ of M by

$$\mathrm{Diam}(M) := \sup_{p,q\in M} \|p-q\|_{\mathbb{R}^\ell}, \quad \mathrm{Curv}(M) := \sup_{p\in M} \sup_{X\in T_pM} \frac{\mathrm{II}_p(X,X)}{\|X\|_{\mathbb{R}^\ell}^2},$$

respectively. If M is compact, then $\mathrm{Diam}(M)$ and $\mathrm{Curv}(M)$ are finite. Given a point $p \in M$ and a velocity $V \in T_pM$, we consider the ordinary differential equation in $\mathbb{R}^\ell$, so-called geodesic equation in M, for $\gamma : [0,\infty) \to \mathbb{R}^\ell$:

$$\frac{\mathrm{d}^2\gamma}{\mathrm{d}t^2}(t) - \mathrm{II}_{\gamma(t)}\left(\frac{\mathrm{d}\gamma}{\mathrm{d}t}(t), \frac{\mathrm{d}\gamma}{\mathrm{d}t}(t)\right) = 0, \quad \gamma(0) = p, \quad \frac{\mathrm{d}\gamma}{\mathrm{d}t}(0) = V. \tag{2.1}$$

If M is compact, then Hopf–Rinow theorem implies that there exists a unique curve $\gamma^{p,V} : [0,\infty) \to M$ satisfying (2.1). The curve $\gamma^{p,V}$ is called geodesic with an initial point p and an initial velocity V. Then the exponential map $\exp_p : T_pM \to M$ at p is defined by the formula $\exp_p(V) := \gamma^{p,V}(1)$. Then, it holds that $\gamma^{p,V}(t) = \exp_p(tV)$ for $t \in [0,\infty)$ since $s \mapsto \gamma^{p,tV}(s/t)$ satisfies the geodisc equation (2.1) and uniqueness of solution of geodesic equation holds. Moreover, set

$$C_M := \sup_{p,q\in M} \frac{\left\|\pi_p^\perp(p-q)\right\|_{\mathbb{R}^\ell}}{\|p-q\|_{\mathbb{R}^\ell}^2}. \tag{2.2}$$

If M is path-connected and compact, then the constant C_M is finite. Actually, the constant C_M is bounded by an explicit constant. In Appendix A, we will explain this constant in detail.

2.2. Finite element spaces

First, we define partitions with rectangles. A family $\Omega_\Delta := \{\Omega_\alpha\}_{\alpha\in\Delta}$ of subsets of Ω is a *rectangular partition* of Ω if Ω_Δ satisfies that

(1) $\mathcal{H}^k\left(\Omega \setminus \bigcup_{\alpha\in\Delta} \Omega_\alpha\right) = 0$;

(2) $\mathcal{H}^k(\Omega_\alpha \cap \Omega_\beta) = 0$ for $\alpha \neq \beta$, $(\alpha, \beta) \in \Delta \times \Delta$;

(3) For each $\alpha \in \Delta$, there exists a rectangle R_α in $\mathbb{R}^k$ such that $\Omega_\alpha = R_\alpha \cap \Omega$.

Given a rectangular partition $\Omega_\Delta := \{\Omega_\Delta\}_{\alpha\in\Delta}$ of Ω, we set

$$v(\Omega_\Delta) := \inf_{\alpha\in\Delta} \mathcal{L}^k(\Omega_\alpha), \quad V(\Omega_\Delta) := \sup_{\alpha\in\Delta} \mathcal{L}^k(\Omega_\alpha). \tag{2.3}$$

Moreover, we denote by $e(\Delta)$ the set of edges associated with Δ defined as

$$e(\Delta) := \left\{ \gamma := \{\alpha, \beta\} \subset \Delta \;\middle|\; \mathcal{H}^{k-1}(\overline{\partial\Omega_\alpha \cap \partial\Omega_\beta}) \neq 0,\ \alpha \neq \beta \right\}.$$

For $\gamma := \{\alpha, \beta\} \in e(\Delta)$, we take a bijection $\mathrm{Sign}_\gamma : \gamma \to \{\pm 1\}$ and set $E_\gamma := \overline{\partial\Omega_\alpha \cap \partial\Omega_\beta}$. Moreover, we define the set $E\Omega_\Delta$ of interior edges in Ω associated with Ω_Δ and the sign $\mathrm{Sign}_{e(\Delta)}$ on $e(\Delta)$ by

$$E\Omega_\Delta := \{E_\gamma\}_{\gamma\in e(\Delta)}, \quad \mathrm{Sign}_{e(\Delta)} := \{\mathrm{Sign}_\gamma\}_{\gamma\in e(\Delta)},$$

respectively.

Subsequently, we define function spaces associated with a rectangular partition of Ω_Δ. Assume that a rectangele partition Ω_Δ of Ω is given. Then, we define a space H_Δ of piecewise constant $\mathbb{R}^\ell$-valued functions on Ω associated with Ω_Δ by

$$H_\Delta := \left\{ U \in L^2(\Omega; \mathbb{R}^\ell) \;\middle|\; U|_{\Omega_\alpha} \text{ is constant for each } \Omega_\alpha \in \Omega_\Delta \right\}.$$

We regard the space H_Δ as a closed linear subspace of the Hilbert space $L^2(\Omega; \mathbb{R}^\ell)$ endowed with the inner product defined by

$$\langle X, Y \rangle_{H_\Delta} := \langle X, Y \rangle_{L^2(\Omega;\mathbb{R}^\ell)}.$$

For $U \in H_\Delta$, we denote the facet of U in H_Δ by

$$\mathrm{Facet}(U) := \{\{\alpha, \beta\} \in e(\Delta) \mid U|_{\Omega_\alpha} = U|_{\Omega_\beta}\}.$$

Moreover, we define a space $H_{E\Omega_\Delta}$ of piecewise constant $\mathbb{R}^\ell$-valued maps on $\bigcup E\Omega_\Delta$ associated with Ω_Δ by

$$H_{E\Omega_\Delta} := \left\{ U \in L^2\left(\bigcup E\Omega_\Delta; \mathbb{R}^\ell\right) \;\middle|\; U|_{E_\gamma} \text{ is constant in } \mathbb{R}^\ell \text{ for each } E_\gamma \in E\Omega_\Delta \right\}.$$

Subsequently, we define a subset M_Δ of H_Δ by

$$M_\Delta := \left\{ u \in L^2(\Omega; M) \;\middle|\; u|_{\Omega_\alpha} \text{ is constant value for each } \Omega_\alpha \in \Omega_\Delta \right\}.$$

for $u \in M_\Delta$, we denote by $T_u M_\Delta$ the tangent space of M_Δ at u, i.e.,

$$T_u M_\Delta := \left\{ X \in L^2(\Omega; \mathbb{R}^\ell) \;\middle|\; X(x) \text{ is in } T_{u(x)}M \text{ for all } x \in \Omega \right\}.$$

We regard the space M_Δ as a submanifold of H_Δ, and the space $T_u M_\Delta$ the tangent space at u of M_Δ. Then orthogonal projections and an exponential map in M_Δ are naturally induced from ones in M as follows. For $u \in M_\Delta$, we define the orthogonal projections $\mathrm{P}_u \colon H_\Delta \to T_u M_\Delta$, $\mathrm{P}_u^\perp \colon H_\Delta \to T_u^\perp M_\Delta$ by

$$(\mathrm{P}_u X)(x) := \pi_{u(x)}(X(x)), \qquad (\mathrm{P}_u^\perp X)(x) := \pi_{u(x)}^\perp(X(x)), \quad \text{for a.e.} \quad x \in \Omega,$$

and define an exponential map $\mathrm{Exp}_u \colon T_u M_\Delta \to M_\Delta$ by

$$(\mathrm{Exp}_u X)(x) := \exp_{u(x)}(X(x)), \quad \text{for a.e.} \quad x \in \Omega,$$

where $\exp_p$ denotes the exponential map of M at $p \in M$.

2.3. Constrained discrete total variation flows

We recall the constrained discrete total variation flow proposed in [18], here. The Neumann problem (TVF; u_0) is formally regarded as the gradient system of (isotropic) total variation:

$$\begin{aligned}\boldsymbol{TV}(u) &:= \int_\Omega |\boldsymbol{D}u| \\ &:= \sup_{\boldsymbol{\varphi}\in\mathcal{A}} \sum_{j=1}^{\ell} \int_\Omega u^j (\nabla\cdot\varphi^j)\,\mathrm{d}x, \quad u := (u^1,\dots,u^\ell) \in L^1(\Omega;\mathbb{R}^\ell),\end{aligned}$$

where

$$\mathcal{A} := \left\{ \boldsymbol{\varphi} := (\varphi^1,\dots,\varphi^\ell) \in C_0^\infty(\Omega;\mathbb{R}^{k\times\ell}) \;\middle|\; \|\boldsymbol{\varphi}\|_{\mathbb{R}^{k\times\ell}} \le 1 \right\}.$$

The spatially discrete problems we consider in this paper are just regarded as the gradient system of *discrete (isotropic) total variation*. Let us begin with the definition of discrete total variation associated with a rectangular partition of Ω.

Let $\Omega_\Delta := \{\Omega_\alpha\}_{\alpha\in\Delta}$ be a rectangular partition of Ω. Then the discrete total variation functional $\boldsymbol{TV}_\Delta \colon H_\Delta \to \mathbb{R}$ associated with Ω_Δ is defined as follows:

$$\boldsymbol{TV}_\Delta(u) := \sum_{\gamma\in e(\Delta)} \|(\boldsymbol{D}_\Delta u)^\gamma\|_{\mathbb{R}^\ell}\, \mathcal{H}^{k-1}(E_\gamma), \tag{2.4}$$

where $\boldsymbol{D}_\Delta (:= \boldsymbol{D}_\Delta^{\mathrm{Sign}_{e(\Delta)}}) : H_\Delta \to H_{E\Omega_\Delta}$ is the discrete gradient associated with Ω_Δ which is defined by

$$\begin{aligned}\boldsymbol{D}_\Delta u &:= \sum_{\{\alpha,\beta\}\in e(\Delta)} (\boldsymbol{D}_\Delta u)^{\{\alpha,\beta\}} \mathbf{1}_{E_{\{\alpha,\beta\}}} \\ &:= \sum_{\{\alpha,\beta\}\in e(\Delta)} (\mathrm{Sign}_{\{\alpha,\beta\}}(\alpha) u^\alpha + \mathrm{Sign}_{\{\alpha,\beta\}}(\beta) u^\beta) \mathbf{1}_{E_{\{\alpha,\beta\}}}, \quad u := \sum_{j\in\Delta} u^j \mathbf{1}_{\Omega_j}.\end{aligned}$$

This definition is easily deduced from the original definition of $\boldsymbol{TV}(u)$ when u is a piecewise constant function associated with Ω_Δ. We remark that the functional $\boldsymbol{TV}_\Delta$ is convex on H_Δ but not differentiable at a point u whose facet $\mathrm{Facet}(u)$ is not empty. The next proposition is immediate conclusion of definition of $\boldsymbol{TV}_\Delta$. Hence, we state this without its proof:

Proposition 2.1. *The following statements hold:*

1. $\boldsymbol{TV}_\Delta$ *is a semi-norm in* H_Δ.
2. $\boldsymbol{TV}_\Delta$ *is Lipschitz continuous on* H_Δ, *that is,*

$$\mathrm{Lip}(\boldsymbol{TV}_\Delta) := \sup_{u,v\in H_\Delta} \frac{|\boldsymbol{TV}_\Delta(u) - \boldsymbol{TV}_\Delta(v)|}{\|u-v\|_{H_\Delta}} < \infty.$$

3. $\boldsymbol{TV}_\Delta(u)$ *is equal to* $\boldsymbol{TV}(u)$ *for all* $u \in H_\Delta$.

Constrained discrete total variation flow (Constrained discrete TV flow for short) is the constrained L^2-gradient flow of spatially discrete total variation. Since the discrete total variation $\boldsymbol{TV}_\Delta$ is not differentiable but convex in H_Δ, we define gradients of constrained discrete TV flows by

$$-\mathrm{P}_u \partial \boldsymbol{TV}_\Delta(u) := \{-\mathrm{P}_u\zeta \mid \zeta \in \partial \boldsymbol{TV}_\Delta(u)\}, \quad u \in M_\Delta, \tag{2.5}$$

where $\partial \boldsymbol{TV}_\Delta$ denotes the subdifferential of $\boldsymbol{TV}_\Delta$ in H_Δ, that is,

$$\partial \boldsymbol{TV}_\Delta(u) := \left\{ \zeta \in H_\Delta \;\middle|\; \langle \zeta, v-u \rangle_{H_\Delta} + \boldsymbol{TV}_\Delta(u) \le \boldsymbol{TV}_\Delta(v) \text{ for all } v \in H_\Delta \right\}, \quad u \in H_\Delta.$$

Then, we define the constrained discrete total variation flow equation:

Definition 2.1 (constrained discrete TV flows)**.** Let M be a submanifold in $\mathbb{R}^\ell$. Let $u_0 \in M_\Delta$ and $I := [0,T)$. A map $u \in C(I; M_\Delta)$ is said to be *a solution to the discrete GK-model of* $(\mathrm{TVF}; u_0)$ if u satisfies $u \in W^{1,2}(I; H_\Delta)$ and

$$(\mathrm{DTVF}_{GK}; u_0) \begin{cases} \dfrac{du}{dt}(t) \in -\mathrm{P}_{u(t)} \partial \boldsymbol{TV}_\Delta(u(t)) \quad \text{for a.e. } t \in (0,T), \\ \\ u|_{t=0} = u_0. \end{cases} \tag{2.6}$$

Here, we note that the existence and the uniqueness of global-in-time solution of the discrete GK-model have been proved in [16, 18, 32]:

Proposition 2.2 ([16, 18, 32])**.** *Let M be a compact submanifold in $\mathbb{R}^\ell$. Let $u_0 \in M_\Delta$ and $I := [0,T)$ be a time interval. Then, there exits a solution $u \in C(I; M_\Delta)$ to the discrete GK-model of $(TVF; u_0)$. Moreover, assuming that M is path-connected, then u is the unique solution of the discrete GK-model of $(TVF; u_0)$.*

3. Proposed scheme and its theoretical properties

In this section, we propose a new numerical scheme based on a minimizing movement scheme and state properties of the proposed scheme, "energy decay" and "error rate".

3.1. Proposed scheme and its derivation

We seek a suitable time-discrete model of a constrained spatial discrete total variation flow equation. Since constrained discrete total variation flows have a structure of constrained gradient flows, we use the minimizing movement scheme in [2] in order to obtain the space-time discrete model. First, we introduce notions and notations. A sequence $\boldsymbol{\tau} := \{\tau^{(n)}\}_{n=0}^N$ be a partition of $I := [0,T)$ if $\boldsymbol{\tau}$ satisfies that

$$0 =: \tau^{(0)} < \tau^{(1)} < \ldots < \tau^{(N-1)} < \tau^{(N)} := T$$

Moreover, $|\boldsymbol{\tau}| := \sup_{n \in \{1,\ldots,N\}} |\tau^{(n)} - \tau^{(n-1)}|$ denotes the maximal width of $\boldsymbol{\tau}$.

Assume that a time partition of time interval $\boldsymbol{\tau} := \{\tau^{(n)}\}_{n=0}^N$ and an initial datum $u_0 \in M_\Delta$ are given. Then a minimizing movement scheme for the discrete GK-model of $(\mathrm{TVF}; u_0)$ is as follows:

Algorithm 3 ($(\mathrm{MMS}; \boldsymbol{\tau}, u_0)$: Minimizing Movement Scheme)**.** *A sequence $\left\{u_{\boldsymbol{\tau}}^{(n)}\right\}_{n=0}^N$ in M_Δ is defined by the following scheme:*

1. *For $n = 0$, $u_{\boldsymbol{\tau}}^{(0)} := u_0$.*
2. *For $n \ge 1$, $u_{\boldsymbol{\tau}}^{(n)}$ is a minimizer of the optimization problem $(\mathrm{OP}; \tau^{(n)} - \tau^{(n-1)}, u_{\boldsymbol{\tau}}^{(n-1)})$:*

$$\textit{Minimize } \Phi(u; \tau^{(n)} - \tau^{(n-1)}, u_{\boldsymbol{\tau}}^{(n-1)}) \textit{ subject to } u \in M_\Delta,$$

where

$$\Phi(u;\tau,v) := \tau\, \boldsymbol{TV}_\Delta(u) + \frac{1}{2}\|u-v\|^2_{H_\Delta}, \quad u,v \in H_\Delta, \quad \tau > 0.$$

We determine $u_{\boldsymbol{\tau}}^{(n)}$ by the optimization problem $(\mathrm{OP};\tau^{(n)}-\tau^{(n-1)},u_{\boldsymbol{\tau}}^{(n-1)})$ when we use the minimizing movements scheme. However, it is not easy to solve the problem $(\mathrm{OP};\tau^{(n)}-\tau^{(n-1)},u_{\boldsymbol{\tau}}^{(n-1)})$ generally since each the problem $(\mathrm{OP};\tau^{(n)}-\tau^{(n-1)},u_{\boldsymbol{\tau}}^{(n-1)})$ is classified as *non-smooth Riemanian constraint optimization problem*. This difficulty motivates us to replace $(\mathrm{OP};\tau^{(n)}-\tau^{(n-1)},u_{\tau}^{(n-1)})$ with an optimization problem easier to handle. Our strategy is to determine $u_{\boldsymbol{\tau}}^{(n)}$ from tangent vector $X \in T_{u_{\boldsymbol{\tau}}^{(n-1)}}M_\Delta$ which is the optimizer of *non-smooth (convex) optimization problem* $(\mathrm{OP}^\dagger;\tau^{(n)}-\tau^{(n-1)},u_{\boldsymbol{\tau}}^{(n-1)})$ *with constraint into the tangent space* $T_{u_{\boldsymbol{\tau}}^{(n-1)}}M_\Delta$ by using the exponential map $\mathrm{Exp}_{u_{\boldsymbol{\tau}}^{(n-1)}} : T_{u_{\boldsymbol{\tau}}^{(n-1)}}M_\Delta \to M_\Delta$.

Let us explain more explicitly. First, we rewrite the optimization problem $(\mathrm{OP};\tau^{(n)}-\tau^{(n-1)},u_{\boldsymbol{\tau}}^{(n-1)})$ to obtain the one with a constraint into the tangent space $X \in T_{u_{\boldsymbol{\tau}}^{(n-1)}}M_\Delta$. Each $u \in M_\Delta$, thanks to the exponential map in M, can be rewritten as the pair of $u_{\boldsymbol{\tau}}^{(n-1)}$ and $X \in T_{u_{\boldsymbol{\tau}}^{(n-1)}}M_\Delta$ such that $u = \mathrm{Exp}_{u_{\boldsymbol{\tau}}^{(n-1)}}(X)$, where $\mathrm{Exp}_{u_{\boldsymbol{\tau}}^{(n-1)}} : T_{u_{\boldsymbol{\tau}}^{(n-1)}}M_\Delta \to M_\Delta$ is defined by

$$X(x) \mapsto \exp_{u_{\boldsymbol{\tau}}^{(n-1)}(x)}(X(x)), \quad \text{for a.e. } x \in \Omega.$$

Since $\mathrm{Exp}_{u_{\boldsymbol{\tau}}^{(n-1)}}(X) = u_{\boldsymbol{\tau}}^{(n-1)} + X + o(X)$, we ignore the term $o(X)$ and insert $u = u_{\boldsymbol{\tau}}^{(n-1)} + X$ into $\Phi(u;\tau^{(n)}-\tau^{(n-1)},u_{\boldsymbol{\tau}}^{(n-1)})$ in $(\mathrm{OP};\tau^{(n)}-\tau^{(n-1)},u_{\boldsymbol{\tau}}^{(n-1)})$ to obtain

$$\Phi(u_{\boldsymbol{\tau}}^{(n-1)}+X;\tau^{(n)}-\tau^{(n-1)},u_{\boldsymbol{\tau}}^{(n-1)}) := (\tau^{(n)}-\tau^{(n-1)})\boldsymbol{TV}_\Delta(u_{\boldsymbol{\tau}}^{(n-1)}+X) + \frac{1}{2}\|X\|^2_{H_\Delta}.$$

Now, we define *the localized energy* $\Phi^\dagger(\cdot;\tau,v) : H_\Delta \to \mathbb{R}, \tau > 0, v \in M_\Delta$ by the formula:

$$\Phi^\dagger(X;\tau,v) = \tau\, \boldsymbol{TV}_\Delta(v+X) + \frac{1}{2}\|X\|^2_{H_\Delta}.$$

Here, we emphasize that $\Phi^\dagger(\cdot;\tau^{(n)}-\tau^{(n-1)},u_{\boldsymbol{\tau}}^{(n-1)})$ is convex in H_Δ since $\boldsymbol{TV}_\Delta$ is convex in H_Δ. Subsequently, we consider the optimization problem $(\mathrm{OP}^\dagger;\tau^{(n)}-\tau^{(n-1)},u_{\boldsymbol{\tau}}^{(n-1)})$:

$$\text{Minimize } \Phi^\dagger(X;\tau^{(n)}-\tau^{(n-1)},u_{\boldsymbol{\tau}}^{(n-1)}) \text{ subject to } X \in T_{u_{\boldsymbol{\tau}}^{(n-1)}}M_\Delta.$$

The problem $(\mathrm{OP}^\dagger;\tau^{(n)}-\tau^{(n-1)},u_{\boldsymbol{\tau}}^{(n-1)})$ is strictly convex because of strict convexity of $\Phi^\dagger(\cdot;\tau^{(n)}-\tau^{(n-1)},u_{\boldsymbol{\tau}}^{(n-1)})$ in the Hilbert space H_Δ and linearity of the space $T_{u_{\boldsymbol{\tau}}^{(n-1)}}M_\Delta$. Hence, we can find a unique minimizer $X_{\boldsymbol{\tau}}^{(n-1)}$ of $(\mathrm{OP}^\dagger;\tau^{(n)}-\tau^{(n-1)},u_{\boldsymbol{\tau}}^{(n-1)})$. Finally, we associate $X_{\boldsymbol{\tau}}^{(n-1)}$ with an element of M_Δ by the formula: $u_{\boldsymbol{\tau}}^{(n)} := \mathrm{Exp}_{u_{\boldsymbol{\tau}}^{(n-1)}}(X_{\boldsymbol{\tau}}^{(n-1)})$. Summarizing the above arguments, we have the following modified minimizing movement scheme $(\mathrm{MMS}^\dagger;\boldsymbol{\tau},u_0)$:

Algorithm 4 ($(\mathrm{MMS}^\dagger;\boldsymbol{\tau},u_0)$: Proposed Scheme)**.** *A sequence* $\left\{u_{\boldsymbol{\tau}}^{(n)}\right\}_{n=0}^N$ *in* M_Δ *is defined by the following procedure:*

1. *For* $n=0$*:* $u_{\boldsymbol{\tau}}^{(0)} := u_0$.
2. *For* $n \geq 1$*:* $u_{\boldsymbol{\tau}}^{(n)}$ *is defined by the following steps:*

(a) Find the minimizer $X_{\boldsymbol{\tau}}^{(n-1)}$ *of the optimization problem* $(\mathrm{OP}^\dagger; \tau^{(n)} - \tau^{(n-1)}, u_{\boldsymbol{\tau}}^{(n-1)})$*:*

$$\text{Minimize } \Phi^\dagger(X; \tau^{(n)} - \tau^{(n-1)}, u_{\boldsymbol{\tau}}^{(n-1)}) \text{ subject to } X \in T_{u_{\boldsymbol{\tau}}^{(n-1)}} M_\Delta,$$

where $\Phi^\dagger(X; \tau, v) : H_\Delta \to \mathbb{R}^1, \tau > 0, v \in M_\Delta$ *is defined by*

$$\Phi^\dagger(\cdot; \tau, v) := \tau\, \boldsymbol{TV}_\Delta(v + X) + \frac{1}{2} \|X\|_{H_\Delta}^2 .$$

(b) Set $u_{\boldsymbol{\tau}}^{(n)} := \mathrm{Exp}_{u_{\boldsymbol{\tau}}^{(n-1)}}(X_{\boldsymbol{\tau}}^{(n-1)})$.

The proposed scheme is always well-defined since the minimizer is unique. Here is the statement:

Proposition 3.1 (Well-definedness of the proposed scheme)**.** *Let* M *be a path-connected and compact submanifold of* $\mathbb{R}^\ell$*. Let* $\boldsymbol{\tau} := \left\{\tau^{(n)}\right\}_{n=0}^N$ *be a time partition of* I *and* $u_0 \in M_\Delta$ *be an initial datum. Then sequences* $\left\{u_{\boldsymbol{\tau}}^{(n)}\right\}_{n=0}^N$, $\left\{X_{\boldsymbol{\tau}}^{(n)}\right\}_{n=0}^{N-1}$ *in the proposed scheme* $(\mathrm{MMS}^\dagger; \boldsymbol{\tau}; u_0)$ *are well-defined, and satisfy*

1. $X_{\boldsymbol{\tau}}^{(n-1)} \in -(\tau^{(n)} - \tau^{(n-1)}) \mathrm{P}_{u_{\boldsymbol{\tau}}^{(n-1)}} \partial \boldsymbol{TV}_\Delta(u_{\boldsymbol{\tau}}^{(n-1)} + X_{\boldsymbol{\tau}}^{(n-1)})$,
2. $\left\|X_{\boldsymbol{\tau}}^{(n-1)}\right\|_{H_\Delta} \le (\tau^{(n)} - \tau^{(n-1)})\ \mathrm{Lip}(\boldsymbol{TV}_\Delta)$

for all $n \in \{1, \dots, N\}$.

Remark 3.1 (Why the proposed scheme describe facet-preserving phenomena)**.** In the numerical calculation of (constrained) total variation flows, we should pay attention to whether the scheme can adequately simulate the evolution of facet of numerical solutions. We would like to briefly explain why this scheme can describe facet-preserving phenomena: Given $u \in M_\Delta$ and $X \in T_u M_\Delta$, the total variation of $u + X$ is decomposed into

$$\begin{aligned}\boldsymbol{TV}_\Delta(u + X) = &\sum_{\partial\Delta \setminus \mathrm{Facet}(u)} \|(\boldsymbol{D}_\Delta(u + X))^\gamma\|_{\mathbb{R}^\ell}\, \mathcal{H}^{k-1}(E_\gamma) \\ &+ \sum_{\gamma \in \mathrm{Facet}(u)} \|(\boldsymbol{D}_\Delta X)^\gamma\|_{\mathbb{R}^\ell}\, \mathcal{H}^{k-1}(E_\gamma).\end{aligned}$$

Hence, the minimizer $X_* \in T_u M_\Delta$ of the optimization problem

$$\text{Minimize} \quad \tau\, \boldsymbol{TV}_\Delta(u + X) + \frac{1}{2} \|X\|_{H_\Delta}^2 \text{ subject to } X \in T_u M_\Delta,$$

tends to have the same facet of u, that is, $\mathrm{Facet}(u) = \mathrm{Facet}(X_*)$. Therefore, $\mathrm{Exp}_u(X_*)$ also tends to have same facet of u.

3.2. Energy decay

Total variation decays along corresponding constrained TV flows. Hence, it is desirable that the proposed scheme also has this property. In fact, the proposed scheme has this property if maximal width is small enough.

Proposition 3.2 (Energy Decay)**.** *Let M be a path-connected and compact submanifold of $\mathbb{R}^\ell$. Let $\boldsymbol{\tau} := \{\tau^{(n)}\}_{n=0}^N$ be a time partition of I and $u_0 \in M_\Delta$ be an initial datum. Let $\left\{u_{\boldsymbol{\tau}}^{(n)}\right\}_{n=0}^N$ be a sequence generated by the proposed scheme* $(\mathrm{MMS}^\dagger; \boldsymbol{\tau}, u_0)$*. If*

$$|\boldsymbol{\tau}|\ \mathrm{Curv}(M) \cdot \mathrm{Lip}(\boldsymbol{TV}_\Delta) \leq 1,$$

then

$$\boldsymbol{TV}_\Delta(u_{\boldsymbol{\tau}}^{(n+1)}) \leq \boldsymbol{TV}_\Delta(u_{\boldsymbol{\tau}}^{(n)})$$

for all $n = 0, \ldots, N-1$.

3.3. Error rate

Here, we state an error rate between sequence generated by $(\mathrm{MMS}^\dagger; \boldsymbol{\tau}, u_0)$ and solutions to the discrete GK-model of $(\mathrm{TVF}; u_0)$ when an initial datum $u_0 \in M_\Delta$ is given.

Theorem 3.1 (Error Rate)**.** *Let M be a path-connected and compact submanifold in $\mathbb{R}^\ell$. Let $I := [0, T)$ be a time interval and $\boldsymbol{\tau} := \{\tau^{(n)}\}_{n=0}^N$ be a time partition of I. Fix two initial data $u_0^1, u_0^2 \in M_\Delta$. Let $u \in C(I; M_\Delta)$ be a solution of the discrete GK-model of* $(\mathrm{TVF}; u_0^1)$ *and $\left\{u_{\boldsymbol{\tau}}^{(n)}\right\}_{n=0}^N$ be a sequence generated by the proposed scheme* $(\mathrm{MMS}^\dagger; \boldsymbol{\tau}, u_0^2)$*. Then,*

$$\left\|u_{\boldsymbol{\tau}}^{(n)} - u(\tau^{(n)})\right\|_{H_\Delta}^2 \leq e^{C_0 \tau^{(n)}} \left\|u_0^1 - u_0^2\right\|_{H_\Delta}^2 + \tau^{(n)} e^{C_0 \tau^{(n)}} (C_1 |\boldsymbol{\tau}| + C_2 |\boldsymbol{\tau}|^2) \tag{3.1}$$

for all $n \in \{0, 1, \ldots, N\}$, where

$$C_0 := 2\ C_M\ v(\Omega_\Delta)^{-1}\ \mathrm{Lip}(\boldsymbol{TV}_\Delta), \tag{3.2}$$

$$C_1 := \left(2 + \frac{\mathrm{Diam}(M_\Delta)\ \mathrm{Curv}(M)}{2} + 2C_M\ \mathrm{Diam}(M_\Delta)\ v(\Omega_\Delta)^{-1}\right)\ \mathrm{Lip}(\boldsymbol{TV}_\Delta)^2, \tag{3.3}$$

$$C_2 := \left(\frac{3}{2}\ \mathrm{Curv}(M) + C_M\ v(\Omega_\Delta)^{-1}\right)\ \mathrm{Lip}(\boldsymbol{TV}_\Delta)^3. \tag{3.4}$$

Remark 3.2. In this theorem, we cannot remove the exponentially growth term $e^{C\tau^{(n)}}$ from the right hand side of (3.1), because the functional $\boldsymbol{TV}_\Delta$ defined by (2.4) is generally semi-convex functional and not convex under manifold constraint.

4. Proof of theoretical properties of the proposed scheme

In this section, we prove Proposition 3.2 and Theorem 3.1.

4.1. Rothe interpolation

We consider the Rothe interpolation of a sequences generated by the proposed scheme. This interpolation is useful to prove energy decay in Proposition 3.2 and convergence rate in Theorem 3.1.

Let $I := [0, T)$ be a time interval, $\boldsymbol{\tau} := \{\tau^{(n)}\}_{n=0}^{N}$ be a partition of I, and $|\boldsymbol{\tau}|$ be the maximal width of $\boldsymbol{\tau}$. Then we define the time interpolation functions $\left\{\ell_{\boldsymbol{\tau}}^{(n)}\right\}_{n=0}^{N-1} : I \to [0, 1)$ of $\boldsymbol{\tau}$ by

$$\ell_{\boldsymbol{\tau}}^{(n)}(t) := \frac{t - \tau^{(n)}}{\tau^{(n+1)} - \tau^{(n)}} 1_{[\tau^{(n)}, \tau^{(n+1)})}(t), \quad t \in I, \quad n \in \{0, 1, \dots, N-1\}. \tag{4.1}$$

Let $u_0 \in M_\Delta$ be a an initial datum. Let $\left\{u_{\boldsymbol{\tau}}^{(n)}\right\}_{n=0}^{N}$ be a sequence generated by the proposed scheme $(\mathrm{MMS}^\dagger; \boldsymbol{\tau}, u_0)$. Then, we define the *Rothe interpolation* $u_{\boldsymbol{\tau}} \colon I \to M_\Delta$ of $\left\{u_{\boldsymbol{\tau}}^{(n)}\right\}_{n=0}^{N}$ as follows:

$$u_{\boldsymbol{\tau}}(t) := \sum_{n=0}^{N-1} \left(\mathrm{Exp}_{u_{\boldsymbol{\tau}}^{(n)}}(\ell_{\boldsymbol{\tau}}^{(n)}(t) X_{\boldsymbol{\tau}}^{(n)})\right) 1_{[\tau^{(n)}, \tau^{(n+1)})}(t), \quad t \in I.$$

Proposition 4.1 (Properties of Rothe interpolation)**.** *Let M be a path-connected and compact submanifold in $\mathbb{R}^\ell$. Let $\boldsymbol{\tau} := \{\tau^{(n)}\}_{n=0}^{N}$ be a time partition of a time interval I and $u_0 \in M_\Delta$ be an initial datum. Let $\left\{u_{\boldsymbol{\tau}}^{(n)}\right\}_{n=0}^{N}$, $\left\{X_{\boldsymbol{\tau}}^{(n)}\right\}_{n=0}^{N-1}$ be sequences in the proposed scheme $(\mathrm{MMS}^\dagger; \boldsymbol{\tau}, u_0)$. Let $u_{\boldsymbol{\tau}}$ be the Rothe interpolation of $\left\{u_{\boldsymbol{\tau}}^{(n)}\right\}_{n=0}^{N}$. Then, for each $n = 0, \dots, N-1$,*

1. *the curve $u_{\boldsymbol{\tau}}|_{[\tau^{(n)}, \tau^{(n+1)})}$ is C^2-smooth,*
2. *the velocity of $u_{\boldsymbol{\tau}}|_{[\tau^{(n)}, \tau^{(n+1)})}$ satisfies*

$$\left\| \frac{\mathrm{d} u_{\boldsymbol{\tau}}|_{[\tau^{(n)}, \tau^{(n+1)})}}{\mathrm{d}t} \right\|_{H_\Delta} = \frac{\left\| X_{\boldsymbol{\tau}}^{(n)} \right\|_{H_\Delta}}{\tau^{(n+1)} - \tau^{(n)}}, \tag{4.2}$$

3. *the acceleration of $u_{\boldsymbol{\tau}}|_{[\tau^{(n)}, \tau^{(n+1)})}$ satisfies that*

$$\left\| \frac{\mathrm{d}^2 u_{\boldsymbol{\tau}}|_{[\tau^{(n)}, \tau^{(n+1)})}}{\mathrm{d}t^2} \right\|_{H_\Delta} \leq \frac{\mathrm{Curv}(M) \cdot \left\| X_{\boldsymbol{\tau}}^{(n)} \right\|_{H_\Delta}^2}{(\tau^{(n+1)} - \tau^{(n)})^2}. \tag{4.3}$$

Proof. Fix $n \in \{1, \dots, N-1\}$.
(1): Since $u_{\boldsymbol{\tau}}|_{[\tau^{(n)}, \tau^{(n+1)})} = \exp_{u_{\boldsymbol{\tau}}^{(n)}}(\ell_{\boldsymbol{\tau}}^{(n)} X_{\boldsymbol{\tau}}^{(n)})$, $u_{\boldsymbol{\tau}}$ is C^2-smooth.
(2): Since a speed of geodesic is constant, we have

$$\left\| \frac{\mathrm{d} u_{\boldsymbol{\tau}}|_{[\tau^{(n)}, \tau^{(n+1)})}}{\mathrm{d}t} \right\|_{H_\Delta} = \left\| \frac{\mathrm{d} u_{\boldsymbol{\tau}}}{\mathrm{d}t}(\tau^{(n)}) \right\|_{H_\Delta} = \frac{\left\| X_{\boldsymbol{\tau}}^{(n)} \right\|_{H_\Delta}}{\tau^{(n+1)} - \tau^{(n)}}.$$

(3): Since $u_{\boldsymbol{\tau}}^{(n)}$ and $u_{\boldsymbol{\tau}}^{(n+1)}$ is joined by exponential map, $u_{\boldsymbol{\tau}}|_{[\tau^{(n)}, \tau^{(n+1)})}$ satisfies the geodesic equation (2.1), that is,

$$\frac{\mathrm{d}^2 u_{\boldsymbol{\tau}}|_{[\tau^{(n)}, \tau^{(n+1)})}}{\mathrm{d}t^2} - \mathrm{II}_{u_{\boldsymbol{\tau}}|_{[\tau^{(n)}, \tau^{(n+1)})}} \left(\frac{\mathrm{d} u_{\boldsymbol{\tau}}|_{[\tau^{(n)}, \tau^{(n+1)})}}{\mathrm{d}t}, \frac{\mathrm{d} u_{\boldsymbol{\tau}}}{\mathrm{d}t}|_{[\tau^{(n)}, \tau^{(n+1)})} \right) = 0,$$

$$u_{\boldsymbol{\tau}}|_{[\tau^{(n)},\tau^{(n+1)})}(\tau^{(n)}) = u_{\boldsymbol{\tau}}^{(n)}, \quad \frac{\mathrm{d}u_{\boldsymbol{\tau}}|_{[\tau^{(n)},\tau^{(n+1)})}}{\mathrm{d}t}(\tau^{(n)}) = \frac{X_{\boldsymbol{\tau}}^{(n)}}{\tau^{(n+1)}-\tau^{(n)}}.$$

Hence, we have

$$\left\| \frac{\mathrm{d}^2 u_{\boldsymbol{\tau}}|_{[\tau^{(n)},\tau^{(n+1)})}}{\mathrm{d}t^2} \right\|_{H_\Delta} = \left\| \mathrm{II}_{u_{\boldsymbol{\tau}}|_{[\tau^{(n)},\tau^{(n+1)})}} \left(\frac{\mathrm{d}u_{\boldsymbol{\tau}}|_{[\tau^{(n)},\tau^{(n+1)})}}{\mathrm{d}t}, \frac{\mathrm{d}u_{\boldsymbol{\tau}}|_{[\tau^{(n)},\tau^{(n+1)})}}{\mathrm{d}t} \right) \right\|_{H_\Delta}.$$

The definition of curvature of M implies that

$$\left\| \frac{\mathrm{d}^2 u_{\boldsymbol{\tau}}|_{[\tau^{(n)},\tau^{(n+1)})}}{\mathrm{d}t^2} \right\|_{H_\Delta} \leq \mathrm{Curv}(M) \left\| \frac{\mathrm{d}u_{\boldsymbol{\tau}}|_{[\tau^{(n)},\tau^{(n+1)})}}{\mathrm{d}t} \right\|_{H_\Delta}^2.$$

The equality (4.2) implies that

$$\left\| \frac{\mathrm{d}^2 u_{\boldsymbol{\tau}}|_{[\tau^{(n)},\tau^{(n+1)})}}{\mathrm{d}t^2}(t) \right\|_{H_\Delta} \leq \frac{\mathrm{Curv}(M) \left\| X_{\boldsymbol{\tau}}^{(n)} \right\|_{H_\Delta}^2}{(\tau^{(n+1)}-\tau^{(n)})^2}.$$

□

4.1.1. Proof of energy decay

We prove Proposition 3.2, here.

Proof. Fix $n \in \{0, \dots, N-1\}$. Then expanding $u_{\boldsymbol{\tau}}^{(n+1)} = \mathrm{Exp}_{u_{\boldsymbol{\tau}}^{(n)}}(X_{\boldsymbol{\tau}}^{(n)})$ in Taylor series implies that

$$u_{\boldsymbol{\tau}}^{(n+1)} = u_{\boldsymbol{\tau}}^{(n)} + X_{\boldsymbol{\tau}}^{(n)} + \int_{\tau^{(n)}}^{\tau^{(n+1)}} (\tau^{(n+1)} - s) \frac{\mathrm{d}^2 u_{\boldsymbol{\tau}}}{\mathrm{d}t^2}(s)\, \mathrm{d}s.$$

The above formula and the triangle inequality imply

$$\boldsymbol{TV}_\Delta(u_{\boldsymbol{\tau}}^{(n+1)}) \leq \boldsymbol{TV}_\Delta(u_{\boldsymbol{\tau}}^{(n)} + X_{\boldsymbol{\tau}}^{(n)}) + \boldsymbol{TV}_\Delta \left(\int_{\tau^{(n)}}^{\tau^{(n+1)}} (\tau^{(n+1)} - s) \frac{\mathrm{d}^2 u_{\boldsymbol{\tau}}}{\mathrm{d}t^2}(s)\, \mathrm{d}s \right).$$

Since $X_{\boldsymbol{\tau}}^{(n)}$ is the minimizer of $(\mathrm{OP}^\dagger; \tau^{(n+1)} - \tau^{(n)}, u_{\boldsymbol{\tau}}^{(n)})$, we have

$$\boldsymbol{TV}_\Delta(u_{\boldsymbol{\tau}}^{(n+1)}) \leq \boldsymbol{TV}_\Delta(u_{\boldsymbol{\tau}}^{(n)}) - \frac{1}{2} \frac{\left\| X_{\boldsymbol{\tau}}^{(n)} \right\|_{H_\Delta}^2}{\tau^{(n+1)}-\tau^{(n)}} + \boldsymbol{TV}_\Delta \left(\int_{\tau^{(n)}}^{\tau^{(n+1)}} (\tau^{(n+1)} - s) \frac{\mathrm{d}^2 u_{\boldsymbol{\tau}}}{\mathrm{d}t^2}(s)\, \mathrm{d}s \right).$$

By applying Lipschitz continuity of $\boldsymbol{TV}_\Delta$ and the Minkowski inequality for integrals, we have

$$\begin{aligned} \boldsymbol{TV}_\Delta(u_{\boldsymbol{\tau}}^{(n+1)}) \leq\ & \boldsymbol{TV}_\Delta(u_{\boldsymbol{\tau}}^{(n)}) \\ & - \frac{1}{2} \frac{\left\| X_{\boldsymbol{\tau}}^{(n)} \right\|_{H_\Delta}^2}{\tau^{(n+1)}-\tau^{(n)}} + \mathrm{Lip}(\boldsymbol{TV}_\Delta) \int_{\tau^{(n)}}^{\tau^{(n+1)}} (\tau^{(n+1)} - s) \left\| \frac{\mathrm{d}^2 u_{\boldsymbol{\tau}}}{\mathrm{d}t^2}(s) \right\|_{H_\Delta} ds. \end{aligned}$$

Proposition 4.1 implies that

$$\begin{aligned} \boldsymbol{TV}_\Delta(u_{\boldsymbol{\tau}}^{(n+1)}) \leq\ & \boldsymbol{TV}_\Delta(u_{\boldsymbol{\tau}}^{(n)}) \\ & - \frac{1}{2} \frac{\left\| X_{\boldsymbol{\tau}}^{(n)} \right\|_{H_\Delta}^2}{\tau^{(n+1)}-\tau^{(n)}} + \frac{1}{2} \mathrm{Lip}(\boldsymbol{TV}_\Delta)\ \mathrm{Curv}(M)\ \left\| X_{\boldsymbol{\tau}}^{(n)} \right\|_{H_\Delta}^2. \end{aligned}$$

Since $|\boldsymbol{\tau}|\ \mathrm{Curv}(M)\ \mathrm{Lip}(\boldsymbol{TV}_\Delta) \leq 1$, we have $\boldsymbol{TV}_\Delta(u_{\boldsymbol{\tau}}^{(n+1)}) \leq \boldsymbol{TV}_\Delta(u_{\boldsymbol{\tau}}^{(n)})$. □

4.1.2. Proof of error rate

We prove Theorem 3.1, here. We immediately see that it suffices to prove the following lemma on the error estimate between the Rothe interpolation $u_{\boldsymbol{\tau}}$ and u to prove Theorem 3.1:

Lemma 4.1 (Error rate of Rothe interpolation)**.** *Let M be a path-connected and compact submanifold in $\mathbb{R}^\ell$. Let $I := [0,T)$ be a time interval and $\boldsymbol{\tau} := \{\tau^{(n)}\}_{n=0}^N$ be a time partition of I. Fix two initial data $u_0^1, u_0^2 \in M_\Delta$. Let $u \in C(I; M_\Delta)$ be a solution of the discrete GK-model of* (TVF; u_0^1) *and $u_{\boldsymbol{\tau}} \in C(I; M_\Delta)$ be the Rothe interpolation of the sequence $\left\{u_{\boldsymbol{\tau}}^{(n)}\right\}_{n=0}^N$ generated by the proposed scheme* (MMS†; $\boldsymbol{\tau}, u_0^2$)*. Then u and $u_{\boldsymbol{\tau}}$ satisfy that*

$$\|u_{\boldsymbol{\tau}}(t) - u(t)\|_{H_\Delta}^2 \le e^{C_0 t} \left\|u_0^1 - u_0^2\right\|_{H_\Delta}^2 + t e^{C_0 t}(C_1|\boldsymbol{\tau}| + C_2|\boldsymbol{\tau}|^2), \tag{4.4}$$

for all $t \in I$, where the constants C_0, C_1, C_2 are the same as Theorem 3.1.

Especially in this theorem, setting $u_0^1 = u_0^2$ in (4.4), we have a *convergence rate*

$$\sup_{t\in I} \|u_{\boldsymbol{\tau}}(t) - u(t)\|_{H_\Delta} \le \sqrt{T e^{C_0 T}(C_1|\boldsymbol{\tau}| + C_2|\boldsymbol{\tau}|^2)}.$$

In particular, we obtain that $u_{\boldsymbol{\tau}}$ converges to u in $C(I; M_\Delta)$ as $|\boldsymbol{\tau}|$ tends to 0.

The key estimates to prove Theorem 4.1 are the *evolution variational inequalities* for $u_{\boldsymbol{\tau}}$ and u. First, we state an evolution variational inequality for $u_{\boldsymbol{\tau}}$:

Proposition 4.2 (EVI for Rothe interpolation)**.** *Let M be a path-connected and compact submanifold in $\mathbb{R}^\ell$. Let $I := [0,T)$ be a time interval and $\boldsymbol{\tau} := \{\tau^{(n)}\}_{n=0}^N$ be a time partition of I. Let $u_0 \in M_\Delta$. Let $u_{\boldsymbol{\tau}} : I \to M_\Delta$ be the Rothe interpolation of a sequence $\left\{u_{\boldsymbol{\tau}}^{(n)}\right\}_{n=0}^N$ generated by the proposed scheme* (MMS†; $\boldsymbol{\tau}, u_0$) *Then for each $v \in M_\Delta$, $u_{\boldsymbol{\tau}}$ satisfies that*

$$\frac{1}{2}\frac{\mathrm{d}}{\mathrm{d}t}\|u_{\boldsymbol{\tau}} - v\|_{H_\Delta}^2 \le \boldsymbol{TV}_\Delta(v) - \boldsymbol{TV}_\Delta(u_{\boldsymbol{\tau}}) + \frac{C_0}{2}\|u_{\boldsymbol{\tau}} - v\|_{H_\Delta}^2 + C_1|\boldsymbol{\tau}| + C_2|\boldsymbol{\tau}|^2 \tag{4.5}$$

for all $t \in I \setminus \boldsymbol{\tau}$, where C_0, C_1, C_2 are the same constant in Theorem 3.1.

Proof. Let $v \in M_\Delta$. Assume that $t \in \left[\tau^{(n)}, \tau^{(n+1)}\right)$ for some $n = 0, \dots, N-1$. In the rest, we argue for fixed time $t \in \left[\tau^{(n)}, \tau^{(n+1)}\right)$ and we do not specify the dependence on time for simplicity of notation.

We will compute $\frac{1}{2}\frac{\mathrm{d}}{\mathrm{d}t}\|u_{\boldsymbol{\tau}} - v\|_{H_\Delta}^2$ by splitting it into a semi-monotone term and an error term. Expanding $\mathrm{d}u_{\boldsymbol{\tau}}/\mathrm{d}t$ in Taylor series implies that

$$\frac{\mathrm{d}u_{\boldsymbol{\tau}}}{\mathrm{d}t} = \frac{X_{\boldsymbol{\tau}}^{(n)}}{\tau^{(n+1)} - \tau^{(n)}} + \int_{\tau^{(n)}}^t \frac{\mathrm{d}^2 u_{\boldsymbol{\tau}}}{\mathrm{d}t^2}(s)\,\mathrm{d}s,$$

and inserting this into

$$\frac{1}{2}\frac{\mathrm{d}}{\mathrm{d}t}\|u_{\boldsymbol{\tau}} - v\|_{H_\Delta}^2 = \left\langle \frac{\mathrm{d}u_{\boldsymbol{\tau}}}{\mathrm{d}t}, u_{\boldsymbol{\tau}} - v \right\rangle_{H_\Delta},$$

then

$$\begin{aligned}\frac{1}{2}\frac{\mathrm{d}}{\mathrm{d}t}\|u_{\boldsymbol{\tau}} - v\|_{H_\Delta}^2 &= \left\langle \frac{X_{\boldsymbol{\tau}}^{(n)}}{\tau^{(n+1)} - \tau^{(n)}}, u_{\boldsymbol{\tau}} - v \right\rangle_{H_\Delta} + \int_{\tau^{(n)}}^t \left\langle \frac{\mathrm{d}^2 u_{\boldsymbol{\tau}}}{\mathrm{d}t^2}(s), u_{\boldsymbol{\tau}} - v \right\rangle_{H_\Delta} \mathrm{d}s \\ &=: \boldsymbol{I} + \boldsymbol{II}.\end{aligned} \tag{4.6}$$

Moreover, we split the term $\boldsymbol{I}$ into a monotone term and a non-monotone term. Proposition 3.1 implies that

$$\boldsymbol{I} = \left\langle -\mathrm{P}_{u_{\boldsymbol{\tau}}^{(n)}} \partial \boldsymbol{TV}_\Delta(u_{\boldsymbol{\tau}}^{(n)} + X_{\boldsymbol{\tau}}^{(n)}), u_{\boldsymbol{\tau}} - v \right\rangle_{H_\Delta}.$$

Self adjointness of $\mathrm{P}_{u_{\boldsymbol{\tau}}^{(n)}}$ and the formula $\mathrm{P}_{u_{\boldsymbol{\tau}}^{(n)}} w = w - \mathrm{P}^{\perp}_{u_{\boldsymbol{\tau}}^{(n)}} w, w \in H_\Delta$ imply that

$$\begin{aligned}\boldsymbol{I} &= \left\langle \partial \boldsymbol{TV}_\Delta(u_{\boldsymbol{\tau}}^{(n)} + X_{\boldsymbol{\tau}}^{(n)}), v - u_{\boldsymbol{\tau}} \right\rangle_{H_\Delta} \\ &\qquad + \left\langle \partial \boldsymbol{TV}_\Delta(u_{\boldsymbol{\tau}} + X_{\boldsymbol{\tau}}^{(n)}), \mathrm{P}^{\perp}_{u_{\boldsymbol{\tau}}^{(n)}}(u_{\boldsymbol{\tau}} - v) \right\rangle_{H_\Delta} \\ &=: \boldsymbol{I}_1 + \boldsymbol{I}_2.\end{aligned} \tag{4.7}$$

We plug equality (4.6) and (4.7) to obtain

$$\frac{1}{2}\frac{\mathrm{d}}{\mathrm{d}t} \|u_{\boldsymbol{\tau}} - v\|_{H_\Delta}^2 = \boldsymbol{I}_1 + \boldsymbol{I}_2 + \boldsymbol{II}. \tag{4.8}$$

We shall estimate $\boldsymbol{I}_1$, $\boldsymbol{I}_2$ and $\boldsymbol{II}$, respectively. We claim that

$$\boldsymbol{I}_1 \le \boldsymbol{TV}_\Delta(v) - \boldsymbol{TV}_\Delta(u_{\boldsymbol{\tau}}) + 2\ \mathrm{Lip}(\boldsymbol{TV}_\Delta)^2 |\boldsymbol{\tau}| + \mathrm{Curv}(M)\ \mathrm{Lip}(\boldsymbol{TV}_\Delta)^3 |\boldsymbol{\tau}|^2, \tag{4.9}$$

$$\begin{aligned}\boldsymbol{I}_2 \le\ & C_M\ v(\Omega_\Delta)^{-1}\ \mathrm{Lip}(\boldsymbol{TV}_\Delta)\ \|v - u_{\boldsymbol{\tau}}\|_{H_\Delta}^2 \\ & + 2\ C_M\ v(\Omega_\Delta)^{-1}\ \mathrm{Diam}(M_\Delta)\ \mathrm{Lip}(\boldsymbol{TV}_\Delta)^2\ |\boldsymbol{\tau}| \\ & + \left(\frac{\mathrm{Curv}(M)}{2} + C_M\ v(\Omega_\Delta)^{-1} \right)\ \mathrm{Lip}(\boldsymbol{TV}_\Delta)^3 |\boldsymbol{\tau}|^2,\end{aligned} \tag{4.10}$$

$$\boldsymbol{II} \le \mathrm{Curv}(M)\ \mathrm{Diam}(M_\Delta)\ \mathrm{Lip}(\boldsymbol{TV}_\Delta)^2\ |\boldsymbol{\tau}|. \tag{4.11}$$

First, we estimate the term $\boldsymbol{I}_1$. Since $v - u_{\boldsymbol{\tau}} = (v - u_{\boldsymbol{\tau}} + u_{\boldsymbol{\tau}}^{(n)} + X_{\boldsymbol{\tau}}^{(n)}) - (u_{\boldsymbol{\tau}}^{(n)} + X_{\boldsymbol{\tau}}^{(n)})$, we have

$$\boldsymbol{I}_1 = \left\langle \partial \boldsymbol{TV}_\Delta(u_{\boldsymbol{\tau}}^{(n)} + X_{\boldsymbol{\tau}}^{(n)}), (v - u_{\boldsymbol{\tau}} + u_{\boldsymbol{\tau}}^{(n)} + X_{\boldsymbol{\tau}}^{(n)}) - (u_{\boldsymbol{\tau}}^{(n)} + X_{\boldsymbol{\tau}}^{(n)}) \right\rangle_{H_\Delta}.$$

Since $\partial \boldsymbol{TV}_\Delta(u_{\boldsymbol{\tau}}^{(n)} + X_{\boldsymbol{\tau}}^{(n)})$ is a subgradient of $\boldsymbol{TV}_\Delta$ at $u_{\boldsymbol{\tau}}^{(n)} + X_{\boldsymbol{\tau}}^{(n)}$, we have

$$\boldsymbol{I}_1 \le \boldsymbol{TV}_\Delta(v - u_{\boldsymbol{\tau}} + u_{\boldsymbol{\tau}}^{(n)} + X_{\boldsymbol{\tau}}^{(n)}) - \boldsymbol{TV}_\Delta(u_{\boldsymbol{\tau}}^{(n)} + X_{\boldsymbol{\tau}}^{(n)}).$$

Since $u_{\boldsymbol{\tau}} = u_{\boldsymbol{\tau}}^{(n)} + \frac{t - \tau^{(n)}}{\tau^{(n+1)} - \tau^{(n)}} X_{\boldsymbol{\tau}}^{(n)} + \int_{\tau^{(n)}}^t (t-s) \frac{\mathrm{d}^2 u_{\boldsymbol{\tau}}}{\mathrm{d}t^2}(s)\, \mathrm{d}s$, we have

$$\begin{aligned}\boldsymbol{I}_1 \le\ & \boldsymbol{TV}_\Delta \left(v + \left(1 - \frac{t - \tau^{(n)}}{\tau^{(n+1)} - \tau^{(n)}} \right) X_{\boldsymbol{\tau}}^{(n)} - \int_{\tau^{(n)}}^t (t-s) \frac{\mathrm{d}^2 u_{\boldsymbol{\tau}}}{\mathrm{d}t^2}(s)\, \mathrm{d}s \right) \\ & - \underline{\boldsymbol{TV}_\Delta \left(u_{\boldsymbol{\tau}} - \left(1 - \frac{t - \tau^{(n)}}{\tau^{(n+1)} - \tau^{(n)}} \right) X_{\boldsymbol{\tau}}^{(n)} - \int_{\tau^{(n)}}^t (t-s) \frac{\mathrm{d}^2 u_{\boldsymbol{\tau}}}{\mathrm{d}t^2}(s)\, \mathrm{d}s \right)}.\end{aligned}$$

Here, we applies the reverse triangle inequality, $\boldsymbol{TV}_\Delta(x - y) \ge |\boldsymbol{TV}_\Delta(x) - \boldsymbol{TV}_\Delta(y)|$ for $x, y \in H_\Delta$, to the underlined part in the above inequality to obtain

$$\begin{aligned}\boldsymbol{I}_1 \le\ & \boldsymbol{TV}_\Delta \left(v + \left(1 - \frac{t - \tau^{(n)}}{\tau^{(n+1)} - \tau^{(n)}} \right) X_{\boldsymbol{\tau}}^{(n)} - \int_{\tau^{(n)}}^t (t-s) \frac{\mathrm{d}^2 u_{\boldsymbol{\tau}}}{\mathrm{d}t^2}(s)\, \mathrm{d}s \right) \\ & - \boldsymbol{TV}_\Delta(u_{\boldsymbol{\tau}}) + \boldsymbol{TV}_\Delta \left(\left(1 - \frac{t - \tau^{(n)}}{\tau^{(n+1)} - \tau^{(n)}} \right) X_{\boldsymbol{\tau}}^{(n)} + \int_{\tau^{(n)}}^t (t-s) \frac{\mathrm{d}^2 u_{\boldsymbol{\tau}}}{\mathrm{d}t^2}(s)\, \mathrm{d}s \right).\end{aligned}$$

The triangle inequality for $\boldsymbol{TV}_\Delta$ implies that

$$\begin{aligned}\boldsymbol{I}_1 \leq \boldsymbol{TV}_\Delta(v) - \boldsymbol{TV}_\Delta(u_{\boldsymbol{\tau}}) \\ + 2\ \boldsymbol{TV}_\Delta\left(\left(1 - \frac{t-\tau^{(n)}}{\tau^{(n+1)}-\tau^{(n)}}\right) X_{\boldsymbol{\tau}}^{(n)}\right) \\ + 2\ \boldsymbol{TV}_\Delta\left(\int_{\tau^{(n)}}^{t} (t-s) \frac{\mathrm{d}^2 u_{\boldsymbol{\tau}}}{\mathrm{d}t^2}(s)\,\mathrm{d}s\right).\end{aligned}$$

Proposition 2.1 implies that

$$\begin{aligned}\boldsymbol{I}_1 \leq \boldsymbol{TV}_\Delta(v) - \boldsymbol{TV}_\Delta(u_{\boldsymbol{\tau}}) \\ + 2\ \mathrm{Lip}(\boldsymbol{TV}_\Delta) \left\| \left(1 - \frac{t-\tau^{(n)}}{\tau^{(n+1)}-\tau^{(n)}}\right) X_{\boldsymbol{\tau}}^{(n)} \right\|_{H_\Delta} \\ + 2\ \mathrm{Lip}(\boldsymbol{TV}_\Delta) \int_{\tau^{(n)}}^{t} (t-s) \left\| \frac{\mathrm{d}^2 u_{\boldsymbol{\tau}}}{\mathrm{d}t^2}(s) \right\|_{H_\Delta} \mathrm{d}s.\end{aligned}$$

Proposition 4.1 implies that

$$\begin{aligned}\boldsymbol{I}_1 \leq \boldsymbol{TV}_\Delta(v) - \boldsymbol{TV}_\Delta(u_{\boldsymbol{\tau}}) \\ + 2\ \mathrm{Lip}(\boldsymbol{TV}_\Delta)^2\ |\boldsymbol{\tau}| + \mathrm{Curv}(M)\ \mathrm{Lip}(\boldsymbol{TV}_\Delta)^3\ |\boldsymbol{\tau}|^2.\end{aligned} \tag{4.12}$$

This is the inequality (4.9).

Next, we estimate the term $\boldsymbol{I}_2$. The Cauchy–Schwarz inequality and Proposition 2.1 imply that

$$\boldsymbol{I}_2 \leq \mathrm{Lip}(\boldsymbol{TV}_\Delta) \cdot \left\| \mathrm{P}^{\perp}_{u_{\boldsymbol{\tau}}^{(n)}} (v - u_{\boldsymbol{\tau}}) \right\|_{H_\Delta}. \tag{4.13}$$

Since $u_{\boldsymbol{\tau}} = u_{\boldsymbol{\tau}}^{(n)} + \frac{t-\tau^{(n)}}{(\tau^{(n+1)}-\tau^{(n)})} X_{\boldsymbol{\tau}}^{(n)} + \int_{\tau^{(n)}}^{t} (t-s) \frac{\mathrm{d}^2 u_{\boldsymbol{\tau}}}{\mathrm{d}t^2}(s)\,\mathrm{d}s$, we have

$$\boldsymbol{I}_2 \leq \mathrm{Lip}(\boldsymbol{TV}_\Delta) \cdot \left\| \mathrm{P}^{\perp}_{u_{\boldsymbol{\tau}}^{(n)}} \left((v - u_{\boldsymbol{\tau}}^{(n)}) - \frac{t-\tau^{(n)}}{(\tau^{(n+1)}-\tau^{(n)})} X_{\boldsymbol{\tau}}^{(n)} - \int_{\tau^{(n)}}^{t} (t-s) \frac{\mathrm{d}^2 u_{\boldsymbol{\tau}}}{\mathrm{d}t^2}(s)\,\mathrm{d}s \right) \right\|_{H_\Delta}.$$

Linearity of $\mathrm{P}^{\perp}_{u_{\boldsymbol{\tau}}^{(n)}}$ and $X_{\boldsymbol{\tau}}^{(n)} \in T_{u_{\boldsymbol{\tau}}^{(n)}} M_\Delta$ imply that

$$\boldsymbol{I}_2 \leq \mathrm{Lip}(\boldsymbol{TV}_\Delta) \cdot \left\| \mathrm{P}^{\perp}_{u_{\boldsymbol{\tau}}^{(n)}} (v - u_{\boldsymbol{\tau}}^{(n)}) - \int_{\tau^{(n)}}^{t} (t-s) \mathrm{P}^{\perp}_{u_{\boldsymbol{\tau}}^{(n)}} \frac{\mathrm{d}^2 u_{\boldsymbol{\tau}}}{\mathrm{d}t^2}(s)\,\mathrm{d}s \right\|_{H_\Delta}.$$

The triangle inequality for the norm of H_Δ, and the Minkowski inequality for integrals imply that

$$\boldsymbol{I}_2 \leq \mathrm{Lip}(\boldsymbol{TV}_\Delta) \cdot \left(\left\| \mathrm{P}^{\perp}_{u_{\boldsymbol{\tau}}^{(n)}} (v - u_{\boldsymbol{\tau}}^{(n)}) \right\|_{H_\Delta} + \int_{\tau^{(n)}}^{t} (t-s) \left\| \mathrm{P}^{\perp}_{u_{\boldsymbol{\tau}}^{(n)}} \frac{\mathrm{d}^2 u_{\boldsymbol{\tau}}}{\mathrm{d}t^2}(s) \right\|_{H_\Delta} \mathrm{d}s \right). \tag{4.14}$$

Here, we split to estimate. First, we focus on the term $\left\| \mathrm{P}^{\perp}_{u_{\boldsymbol{\tau}}^{(n)}} (v - u_{\boldsymbol{\tau}}^{(n)}) \right\|_{H_\Delta}$ in (4.14). The inequality (2.2) implies that

$$\left\| \mathrm{P}^{\perp}_{u_{\boldsymbol{\tau}}^{(n)}} (v - u_{\boldsymbol{\tau}}^{(n)}) \right\|_{H_\Delta} \leq C_M \left\| v - u_{\boldsymbol{\tau}}^{(n)} \right\|^2_{L^4(\Omega;\mathbb{R}^\ell)}, \tag{4.15}$$

where C_M is a constant which appears in (2.2). Moreover, monotonicity of the norms $L^p, 1 \leq p \leq \infty$ implies that

$$\left\| \mathrm{P}^{\perp}_{u_{\boldsymbol{\tau}}^{(n)}}(v - u_{\boldsymbol{\tau}}^{(n)}) \right\|_{H_\Delta} \leq C_M v(\Omega_\Delta)^{-1} \left\| v - u_{\boldsymbol{\tau}}^{(n)} \right\|_{H_\Delta}^2, \tag{4.16}$$

where $v(\Omega_\Delta)$ is defined as (2.3). We split $v - u_{\boldsymbol{\tau}}^{(n)} = v - u_{\boldsymbol{\tau}} + u_{\boldsymbol{\tau}} - u_{\boldsymbol{\tau}}^{(n)}$ and use bilineality of the inner product of H_Δ to obtain

$$\begin{aligned}\left\| \mathrm{P}^{\perp}_{u_{\boldsymbol{\tau}}^{(n)}}(v - u_{\boldsymbol{\tau}}^{(n)}) \right\|_{H_\Delta} \leq C_M v(\Omega_\Delta)^{-1} (&\|v - u_{\boldsymbol{\tau}}\|_{H_\Delta}^2 \\ &- 2 \left\langle v - u_{\boldsymbol{\tau}}, u_{\boldsymbol{\tau}} - u_{\boldsymbol{\tau}}^{(n)} \right\rangle_{H_\Delta} + \left\| u_{\boldsymbol{\tau}} - u_{\boldsymbol{\tau}}^{(n)} \right\|_{H_\Delta}^2).\end{aligned}$$

The Cauchy–Schwarz inequality and the definition of the diameter of submanifolds imply that

$$\begin{aligned}\left\| \mathrm{P}^{\perp}_{u_{\boldsymbol{\tau}}^{(n)}}(v - u_{\boldsymbol{\tau}}^{(n)}) \right\|_{H_\Delta} \leq C_M v(\Omega_\Delta)^{-1} (&\|v - u_{\boldsymbol{\tau}}\|_{H_\Delta}^2 \\ &+ 2 \ \mathrm{Diam}(M_\Delta) \left\| u_{\boldsymbol{\tau}} - u_{\boldsymbol{\tau}}^{(n)} \right\|_{H_\Delta} + \left\| u_{\boldsymbol{\tau}} - u_{\boldsymbol{\tau}}^{(n)} \right\|_{H_\Delta}^2).\end{aligned}$$

Since $u_{\boldsymbol{\tau}} = u_{\boldsymbol{\tau}}^{(n)} + \int_{\tau^{(n)}}^t \frac{\mathrm{d}u_{\boldsymbol{\tau}}}{\mathrm{d}s} ds$, we have

$$\begin{aligned}\left\| \mathrm{P}^{\perp}_{u_{\boldsymbol{\tau}}^{(n)}}(v - u_{\boldsymbol{\tau}}^{(n)}) \right\|_{H_\Delta} \leq C_M v(\Omega_\Delta)^{-1} (&\|v - u_{\boldsymbol{\tau}}\|_{H_\Delta}^2 \\ &+ 2 \ \mathrm{Diam}(M_\Delta) \left\| \int_{\tau^{(n)}}^t \frac{\mathrm{d}u_{\boldsymbol{\tau}}}{\mathrm{d}t} ds \right\|_{H_\Delta} + \left\| \int_{\tau^{(n)}}^t \frac{\mathrm{d}u_{\boldsymbol{\tau}}}{\mathrm{d}t} ds \right\|_{H_\Delta}^2).\end{aligned}$$

The Minkowski inequality for integrals, Proposition 4.1 and Proposition 3.1 imply that

$$\begin{aligned}\left\| \mathrm{P}^{\perp}_{u_{\boldsymbol{\tau}}^{(n)}}(v - u_{\boldsymbol{\tau}}^{(n)}) \right\|_{H_\Delta} \leq C_M v(\Omega_\Delta)^{-1} (&\|v - u_{\boldsymbol{\tau}}\|_{H_\Delta}^2 \\ &+ 2 \ |\boldsymbol{\tau}| \ \mathrm{Lip}(\boldsymbol{TV}_\Delta) \ \mathrm{Diam}(M_\Delta) \, |\boldsymbol{\tau}|^2 \ \mathrm{Lip}(\boldsymbol{TV}_\Delta)^2).\end{aligned} \tag{4.17}$$

Next, we focus on the term $\int_{\tau^{(n)}}^t (t-s) \left\| \mathrm{P}^{\perp}_{u_{\boldsymbol{\tau}}^{(n)}} \frac{\mathrm{d}^2 u_{\boldsymbol{\tau}}}{\mathrm{d}t^2}(s) \right\|_{H_\Delta} \mathrm{d}s$ in (4.14). Since the operator norm in H_Δ of $\mathrm{P}^{\perp}_{u_{\boldsymbol{\tau}}^{(n)}}$ is bounded by 1, we have

$$\int_{\tau^{(n)}}^t (t-s) \left\| \mathrm{P}^{\perp}_{u_{\boldsymbol{\tau}}^{(n)}} \frac{\mathrm{d}^2 u_{\boldsymbol{\tau}}}{\mathrm{d}t^2}(s) \right\|_{H_\Delta} \mathrm{d}s \leq \int_{\tau^{(n)}}^t (t-s) \left\| \frac{\mathrm{d}^2 u_{\boldsymbol{\tau}}}{\mathrm{d}t^2}(s) \right\|_{H_\Delta} \mathrm{d}s.$$

Proposition 4.1 and Proposition 3.1 imply that

$$\int_{\tau^{(n)}}^t (t-s) \left\| \mathrm{P}^{\perp}_{u_{\boldsymbol{\tau}}^{(n)}} \frac{\mathrm{d}^2 u_{\boldsymbol{\tau}}}{\mathrm{d}t^2}(s) \right\|_{H_\Delta} \mathrm{d}s \leq \frac{\mathrm{Curv}(M) \cdot \mathrm{Lip}(\boldsymbol{TV}_\Delta)^2}{2} |\boldsymbol{\tau}|^2. \tag{4.18}$$

We plug the inequalities (4.13), (4.17) and (4.18) to obtain the inequality (4.10).

Next, we estimate the term $\boldsymbol{II}$. The Cauchy–Schwarz inequality and the Minkowski inequality for integrals imply that

$$\boldsymbol{II} \leq \mathrm{Diam}(M_\Delta) \int_{\tau^{(n)}}^t \left\| \frac{\mathrm{d}^2 u_{\boldsymbol{\tau}}}{\mathrm{d}t^2}(s) \right\|_{H_\Delta} \mathrm{d}s.$$

Proposition 4.1 and Proposition 3.1 imply that

$$\boldsymbol{II} \leq \mathrm{Curv}(M)\ \mathrm{Diam}(M_\Delta)\ \mathrm{Lip}(\boldsymbol{TV}_\Delta)^2\ |\boldsymbol{\tau}|.$$

This is the inequality (4.11).

Finally, we combine inequalities (4.8), (4.9), (4.10) and (4.11) to obtain

$$\frac{1}{2}\frac{\mathrm{d}}{\mathrm{d}t}\left\|u_{\boldsymbol{\tau}}-v\right\|_{H_\Delta}^2 \leq \boldsymbol{TV}_\Delta(v)-\boldsymbol{TV}_\Delta(u_{\boldsymbol{\tau}})+\frac{C_0}{2}\left\|u_{\boldsymbol{\tau}}-v\right\|_{H_\Delta}^2+C_1|\boldsymbol{\tau}|+C_2|\boldsymbol{\tau}|^2,$$

where C_0, C_1 and C_2 are given in (3.2), (3.3) and (3.4), respectively, which completes the proof. □

Next, we state a evolution variational inequality for solution u to the discrete GK-model of $(\mathrm{TVF};u_0)$:

Proposition 4.3 (EVI for solutions)**.** *Let M be a path-connected and compact submanifold in $\mathbb{R}^\ell$. Let $I:=[0,T)$ be a time interval. Let $u_0\in M_\Delta$. For each $v\in M_\Delta$, a solution $u\in C(I;M_\Delta)$ of the discrete GK-model of* $(\mathrm{TVF};u_0)$ *satisfies*

$$\frac{1}{2}\frac{\mathrm{d}}{\mathrm{d}t}\left\|u-v\right\|_{H_\Delta}^2 \leq \boldsymbol{TV}_\Delta(v)-\boldsymbol{TV}_\Delta(u)+\frac{C_0}{2}\left\|u-v\right\|_{H_\Delta}^2 \tag{4.19}$$

for a.e. $t\in(0,T)$, where C_0 is the same constant in Proposition 4.2.

We omit a proof of Proposition 4.3 since it is proved by a simple argument of proof of Proposition 4.2. Now, we will finish the proof of Lemma 4.1.

Proof of Lemma 4.1: Fix $t\in(0,T)$. By substituting $v=u_{\boldsymbol{\tau}}(t)$ into (4.19) and $v=u(t)$ into (4.5) and adding these two inequality, we obtain

$$\frac{\mathrm{d}}{\mathrm{d}t}\left\|u(t)-u_{\boldsymbol{\tau}}(t)\right\|_{H_\Delta}^2 \leq C_0\left\|u(t)-u_{\boldsymbol{\tau}}(t)\right\|_{H_\Delta}^2+C_1|\boldsymbol{\tau}|+C_2|\boldsymbol{\tau}|^2,$$

where C_1 and C_2 are given in (3.3) and (3.4), respectively. By the Gronwall's inequality, we have

$$\left\|u_{\boldsymbol{\tau}}(t)-u(t)\right\|_{H_\Delta}^2 \leq e^{tC_0}(\left\|u_{\boldsymbol{\tau}}(0)-u(0)\right\|_{H_\Delta}^2+t(C_1|\boldsymbol{\tau}|+C_2|\boldsymbol{\tau}|^2))$$

for all $t\in[0,T)$, which proves Lemma 4.1. □

5. Numerical results

In this section, we show the numerical results by the proposed scheme.

5.1. The proposed scheme with alternating split Bregman iteration

In order to perform the proposed scheme, we need to solve the minimization problem in each iteration. We rewrite the proposed scheme to the one with alternating split Bregman iteration which includes the simpler optimization problems. Let us recall the proposed scheme.

Let $\boldsymbol{\tau}:=\left\{\tau^{(n)}\right\}_{n=0}^N$ be a partiation of a time interval $I:=[0,T)$ and $u_0\in M_\Delta$.

Algorithm 5 ((MMS†; $\boldsymbol{\tau}, u_0$): Proposed Scheme)**.** *A sequence* $\left\{u_{\boldsymbol{\tau}}^{(n)}\right\}_{n=0}^{N}$ *in* M_Δ *is defined by the following procedure:*

1. *For* $n = 0$*:* $u_{\boldsymbol{\tau}}^{(0)} := u_0$.
2. *For* $n \geq 1$*:* $u_{\boldsymbol{\tau}}^{(n)}$ *is defined by the following steps:*
   (a) *Find the minimizer* $X_{\boldsymbol{\tau}}^{(n-1)} \in T_{u_{\boldsymbol{\tau}}^{(n-1)}} M_\Delta$ *of the optimization problem* (OP†; $\tau^{(n)} - \tau^{(n-1)}, u_{\boldsymbol{\tau}}^{(n-1)}$)*:*

$$\textit{Minimize } \Phi^\dagger(X; \tau^{(n)} - \tau^{(n-1)}, u_{\boldsymbol{\tau}}^{(n-1)}) \textit{ subject to } X \in T_{u_{\boldsymbol{\tau}}^{(n-1)}} M_\Delta,$$

   where $\Phi^\dagger(X; \tau, v) := \tau\, \boldsymbol{TV}_\Delta(v + X) + \frac{1}{2} \|X\|_{H_\Delta}^2$.
   (b) *Set* $u_{\boldsymbol{\tau}}^{(n)} = \mathrm{Exp}_{u_{\boldsymbol{\tau}}^{(n-1)}}(X_{\boldsymbol{\tau}}^{(n-1)})$.

We replace the optimization problem (OP†; $\tau^{(n)} - \tau^{(n-1)}, u_{\boldsymbol{\tau}}^{(n-1)}$) to one with alternating split Bregman iteration which is proposed in [21] to solve the L^1 regularization problem efficiently.

First, we apply a splitting method to (OP†; $\tau^{(n)} - \tau^{(n-1)}, u_{\boldsymbol{\tau}}^{(n-1)}$), and we obtain the split formulation (OP‡; $\tau^{(n)} - \tau^{(n-1)}, u_{\boldsymbol{\tau}}^{(n-1)}$):

$$\min_{X \in H_0, Z \in H_1} \Phi^\ddagger(X, Z; \tau^{(n)} - \tau^{(n-1)}, u_{\boldsymbol{\tau}}^{(n-1)}) \text{ subject to } Z = \mathcal{W}(X) + Y(u_{\boldsymbol{\tau}}^{(n-1)}),$$

where $\Phi^\ddagger(\cdot, \cdot; \tau, v) : H_0 \times H_1 \to \mathbb{R} \cup \{\infty\}$, $\tau > 0, v \in M_\Delta$ is defined by

$$\Phi^\ddagger(X, Z; \tau, v) := \tau \left(\|Z_0\|_{L^1\left(\cup E\Omega_\Delta; \mathbb{R}^\ell\right)} + I_{T_v M_\Delta}(Z_1) \right) + \frac{1}{2} \|X\|_{H_\Delta}^2,$$

$$I_{T_v M_\Delta}(X) := \begin{cases} 0, & \text{if } X \in T_v M_\Delta, \\ \infty, & \text{otherwise,} \end{cases}$$

$$\mathcal{W}(X) := \begin{pmatrix} \boldsymbol{D}_\Delta X \\ X \end{pmatrix}, \quad Y(v) := \begin{pmatrix} \boldsymbol{D}_\Delta v \\ 0 \end{pmatrix}, \quad Z = \begin{pmatrix} Z_0 \\ Z_1 \end{pmatrix},$$

in which $H_0 := H_\Delta$ and $H_1 := H_{E\Omega_\Delta} \times H_\Delta$. Subsequently, we apply Bregman iteration with alternating minimization method to (OP‡; $\tau^{(n)} - \tau^{(n-1)}, u_{\boldsymbol{\tau}}^{(n-1)}$), and we obtain the following alternating split Bregman iteration of (OP†; $\tau^{(n)} - \tau^{(n-1)}, u_{\boldsymbol{\tau}}^{(n-1)}$):

Algorithm 6 ((OP‡; $\tau^{(n)} - \tau^{(n-1)}, u_{\boldsymbol{\tau}}^{(n-1)}$): Optimization with Alternating Split Bregman Iteration)**.** *Set* $X_{\boldsymbol{\tau}}^{(n-1)} := \lim_{k \to \infty} X^{(k)}$*, where the sequence* $\left\{X^{(k)}\right\}_{k=0}^{\infty}$ *is defined by the following procedure:*

1. *For* $k = 0$*: Set* $X^{(0)} \in H_0$*,* $Z^{(0)} \in H_1$*,* $B^{(0)} \in H_1$ *and* $\rho > 0$.
2. *For* $k \geq 1$*:*
   (a) $X^{(k)} := \arg\min_{X \in H_0} \Phi_\rho^\ddagger \left(X, Z^{(k-1)}, B^{(k-1)}; \tau^{(n)} - \tau^{(n-1)}, u_{\boldsymbol{\tau}}^{(n-1)} \right)$,
   (b) $Z^{(k)} := \arg\min_{Z \in H_1} \Phi_\rho^\ddagger \left(X^{(k)}, Z, B^{(k-1)}; \tau^{(n)} - \tau^{(n-1)}, u_{\boldsymbol{\tau}}^{(n-1)} \right)$,

(c) $B^{(k)} := B^{(k-1)} + \mathcal{W}(X^{(k)}) + Y(u_{\boldsymbol{\tau}}^{(n-1)}) - Z^{(k)}$.

Here, $\Phi_\rho^\ddagger(\cdot,\cdot,\cdot;\tau,v) : H_0 \times H_1 \times H_1 \to \mathbb{R} \cup \{\infty\}$ $\tau > 0, v \in M_\Delta$ *is defined by*

$$\Phi_\rho^\ddagger(X,Z,B;\tau,v) := \Phi^\ddagger(X,Z;\tau,v) + \frac{\rho}{2}\|Z - \mathcal{W}(X) - Y(v) - B\|_{H_1}^2.$$

Here, we note that

- both $X^{(k)}$ and $Z^{(k)}$ in the above iterations are solved explicitly when the orthogonal projections and the exponential map in M have explicit formulae. The orthogonal projection and the exponential map of an orthogonal Stiefel manifold are written explicitly. S^2 and $SO(3)$ are in class of orthogonal Stiefel manifolds.
- $X^{(k)}$ converges to the minimizer of $(\mathrm{OP}^\dagger; \tau^{(n)} - \tau^{(n-1)}, u_{\boldsymbol{\tau}}^{(n-1)})$ in H_0 thanks to Corollary 2.4.10 in [31].

Finally, we state the proposed scheme with alternating split Bregman iteration:

Algorithm 7 ($(\mathrm{MMS}^\ddagger; \boldsymbol{\tau}, u_0)$: Proposed Scheme with Alternating Split Bregman iteration)**.** *A sequence* $\left\{u_{\boldsymbol{\tau}}^{(n)}\right\}_{n=0}^N$ *in* M_Δ *is defined by the following procedure:*

1. *For* $n = 0$*:* $u_{\boldsymbol{\tau}}^{(0)} := u_0$.
2. *For* $n \geq 1$*:* $u_{\boldsymbol{\tau}}^{(n)}$ *is defined by the following steps:*
   (a) *Set* $X_{\boldsymbol{\tau}}^{(n-1)} := \lim_{k\to\infty} X^{(k)} \in T_{u_{\boldsymbol{\tau}}^{(n-1)}} M_\Delta$*, where the sequence* $\left\{X^{(k)}\right\}_{k=0}^\infty$ *is defined by the following procedure:*
      i. *For* $k = 0$*: Set* $X^{(0)} \in H_0$*,* $Z^{(0)} \in H_1$ *and* $B^{(0)} \in H_1$.
      ii. *For* $k \geq 1$*: Set* $\rho > 0$.
         A. $X^{(k)} := \underset{X\in H_0}{\arg\min}\, \Phi_\rho^\ddagger\left(X, Z^{(k-1)}, B^{(k-1)}; \tau^{(n)} - \tau^{(n-1)}, u_{\boldsymbol{\tau}}^{(n-1)}\right)$,
         B. $Z^{(k)} := \underset{Z\in H_1}{\arg\min}\, \Phi_\rho^\ddagger\left(X^{(k)}, Z, B^{(k-1)}; \tau^{(n)} - \tau^{(n-1)}, u_{\boldsymbol{\tau}}^{(n-1)}\right)$,
         C. $B^{(k)} := B^{(k-1)} + \mathcal{W}(X^{(k)}) + Y(u_{\boldsymbol{\tau}}^{(n-1)}) - Z^{(k)}$.
   (b) *Set* $u_{\boldsymbol{\tau}}^{(n)} = \mathrm{Exp}_{u_{\boldsymbol{\tau}}^{(n-1)}}(X_{\boldsymbol{\tau}}^{(n-1)})$.

5.2. Numerical example (1): $M = S^2$

5.2.1. The tangent spaces, orthogonal projections and exponential maps of S^2

We regard the 2-sphere as $S^2 := \{(x_1,x_2,x_3) \in \mathbb{R}^3 \mid x_1^2 + x_2^2 + x_3^2 = 1\}$. Then the tangent spaces, their orthogonal projections and exponential maps in S^2 are given by the following explicit formulae:

$$\begin{aligned} T_xS^2 &= \{v \in \mathbb{R}^3 \mid \langle x, v\rangle_{\mathbb{R}^3} = 0\}, \\ \pi_x(v) &= (I_{\mathbb{R}^3} - x \otimes x)v, \\ \exp_x(v) &= \exp(v \otimes x - x \otimes v)x, \end{aligned}$$

where $I_{\mathbb{R}^3}$ denotes the identity matrix in $\mathbb{R}^3$ and exp denotes the matrix exponential.

5.2.2. Euler angles

A vector on S^2 has three components. However, since the dimension of S^2 is two, it should be represented by two parameter. Euler angle representation is very useful to describe vectors on S^2. Given $\gamma := (x, y, z) \in S^2$, its Euler angle representation is given as follows:

$$(x, y, z) := (\sin\theta\cos\phi, \sin\theta\sin\phi, \cos\theta),$$

where $(\theta, \phi) \in [0, \pi) \times [0, 2\pi)$ are the Euler angles of γ which are given by the formula

$$(\theta, \phi) := \left(\arccos(z),\ \operatorname{sign}(y)\arccos\left(\frac{x}{\sqrt{x^2+y^2}}\right)\right). \tag{5.1}$$

5.2.3. Counterexample of finite stopping phenomena

In [20], the example of constrained TV flow which does not reach the stationary point in finite time is shown. Here is the statement.

Theorem 5.1 ([20])**.** *Let $a, b \in S^2$ be two points represented by $a = (a_1, a_2, 0)$ and $b = (a_1, -a_2, 0)$ for some $a_1, a_2 \in [-1, 1]$ with $a_1^2 + a_2^2 = 1$ and $a_1 > 0$. Take arbitrary $h_0 \in S^2 \cap \{x_2 = 0\}$ whose x_3-coordinate does not vanish. Then for any $L > 0$ and $0 < \ell_1 < \ell_2 < L$, the constrained TV flow $u : [0, \infty) \to L^2((0, L); S^2)$ starting from the initial value*

$$u_0 = a1_{(0,\ell_1)} + h_0 1_{(\ell_1,\ell_2)} + b1_{(\ell_2,L)}$$

can be represented as

$$u(t) = a1_{(0,\ell_1)} + h(t)1_{(\ell_1,\ell_2)} + b1_{(\ell_2,L)} \tag{5.2}$$

and $h(t)$ converges to $(1, 0, 0)$ as $t \to \infty$ but does not reach it in finite time.

In this theorem, $h(t) = (h_1(t), 0, h_3(t))$ satisfies the following differential equations:

$$\frac{\mathrm{d}}{\mathrm{d}t}(h_1, h_3) = -\frac{\sqrt{2}a_1}{c\sqrt{1 - a_1 h_1}}\left(h_1^2 - 1, h_1 h_3\right), \tag{5.3}$$

and then this can be calculated numerically. Therefore we use it as a benchmark of the validation of our calculation.

Remark 5.1 (Dirichlet problem)**.** So far, in this paper, we have considered the Neumann problem of constrained TV flows. This example is a solution to the Dirichlet problem. Therefore, we can not apply the proposed scheme directly. However, we can lead the Dirichlet problem version of the proposed scheme with a little change. Actually, in the scheme, it is enough to replace $T_{u_\tau^{(n)}} M_\Delta$ with

$$V(u_\tau^{(n)}) := \left\{ X \in T_{u_\tau^{(n)}} M_\Delta \;\middle|\; X|_{\Omega_\alpha} = 0 \text{ for } \alpha \in \partial\Delta \right\},$$

where

$$\partial\Delta := \left\{ \alpha \in \Delta \;\middle|\; \mathcal{H}^{k-1}(\overline{\partial\Omega_\alpha} \cap \overline{\partial\Omega}) \neq 0 \right\}.$$

For a formulation of the Dirichlet problem and its result, see [16, 18, 20]. We emphasize that Proposition 3.2 and Theorem 3.1 hold in the case of the Dirichlet problem.

5.2.4. Setting

We use the following initial data u with the Euler angles $\theta, \phi : (0,1) \times (0,1) \to \mathbb{R}$.

$$\theta := \sum_{i=0}^{2} \boldsymbol{\theta}_i \mathbf{1}_{I_i}, \quad \phi := \sum_{i=0}^{2} \boldsymbol{\phi}_i \mathbf{1}_{I_i}, \tag{5.4}$$

where

$$\boldsymbol{\theta} = \left(\frac{\pi}{2}, \frac{\pi}{4}, \frac{\pi}{2}\right), \quad \boldsymbol{\phi} = \left(\frac{\pi}{4}, \frac{\pi}{2}, \frac{3}{4}\pi\right),$$

and

$$I_0 = \left(0, \frac{2}{5}\right), \quad I_1 = \left(\frac{2}{5}, \frac{3}{5}\right), \quad I_2 = \left(\frac{3}{5}, 1\right).$$

We define the initial value a, b, h as

$$a = \left(\frac{1}{\sqrt{2}}, \frac{1}{\sqrt{2}}, 0\right), \ b = \left(-\frac{1}{\sqrt{2}}, \frac{1}{\sqrt{2}}, 0\right), \ h_0 = \left(0, \frac{1}{\sqrt{2}}, \frac{1}{\sqrt{2}}\right)$$

and compare the results of our scheme with the one calculated from (5.2) and (5.3) when $|\boldsymbol{\tau}| = 10^{-1}, 10^{-2}, 10^{-3}, 10^{-4}$. We set the number of divisions in $[0,1]$ as 100 and used the explicit Euler method to solve the ordinary differential equation (5.3) with time width 10^{-6}.

As we can see from Figure 1, the behavior of the approximate solution computed by our proposed scheme and the one of the solution for (5.3) look similar. Figure 2 depicts the $\log|\boldsymbol{\tau}|$-$\log\|u_{\boldsymbol{\tau}}(t) - u(t)\|_{H_\Delta}$ graph at time $t = 1.0$. We can see from this graph that the L^2 error decreases with the order $O(|\boldsymbol{\tau}|)$ as $|\boldsymbol{\tau}|$ tends to 0 and it is faster than the $O(\sqrt{|\boldsymbol{\tau}|})$-error estimate in Theorem 3.1, which suggests to us that our error estimate has the room for improvement.

5.3. Numerical example (2): $M = SO(3)$

5.3.1. The tangent spaces, orthogonal projections and exponential maps of $SO(3)$

Let $M(3)$ denotes the linear space of all three-by-three matrices, which is a nine-dimensional Hilbert space. Let

$$SO(3) := \left\{ x \in M(3) \;\middle|\; x^\top x = x x^\top = I_{\mathbb{R}^3} \right\},$$

where $I_{\mathbb{R}^3}$ denotes the identity matrix. Then $SO(3)$ is regarded as a matrix Lie group in $M(3)$. The corresponding Lie algebra to $SO(3)$ is given by the all three-dimensional skew symmetric matrices:

$$so(3) := \left\{ X \in M(3) \;\middle|\; X^\top = -X \right\}.$$

According to the general theory of Lie group, $so(3)$ can be regarded as the tangent space $T_{I_{\mathbb{R}^3}}(SO(3))$ at the identity and that

$$so_x(3) := T_x(SO(3)) = \{xX \mid X \in so(3)\}.$$

Hence the exponential map can be given in the following simple form:

$$\exp_x(X) := x \exp(x^\top X), \quad X \in so_x(3),$$

where exp denotes the matrix exponential. For arbitrarily fixed $x \in SO(3)$, the orthogonal projection $\pi_x \colon M(3) \to so_x(3)$ is given by

$$\pi_x(X) := \frac{X - x X^\top x}{2}, \quad X \in SO(3). \tag{5.5}$$

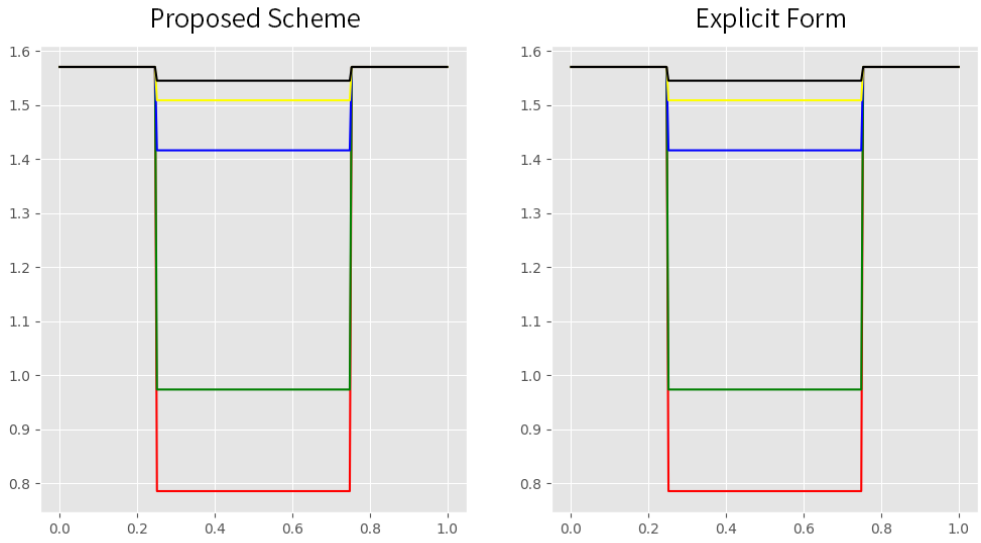

Figure 1: Comparison of flows at $t = 0.0,\ 0.1,\ 0.5,\ 0.75,\ 1.0$: The vertical axis represents the Euler angle θ of the flow. The left side is computed by our scheme, and the right side is computed by using explicit form in [20].

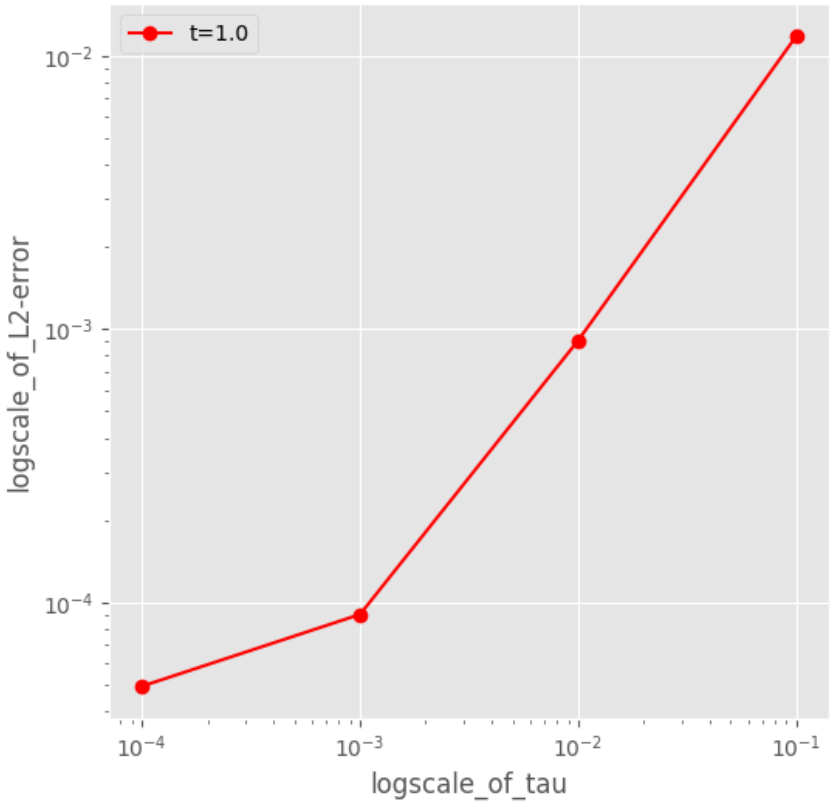

Figure 2: The L^2-error between our numerical scheme and the result in [20] at $t = 1.0$ with respect to the time width $|\boldsymbol{\tau}|$.

5.3.2. Euler angle

A rotation matrix in $\mathbb{R}^3$ have nine components. However, since the dimension of $SO(3)$ is three, it should be represented by three parameters. The Euler angle (or Euler axis) representations are very useful to describe each rotation matrix. Given $R := (R_{i,j})_{i,j=1}^3 \in SO(3)$, its Euler angle (or Euler axis) representation is given by Rodrigues' rotation formula

$$R = \cos\theta I_{\mathbb{R}^3} + (1-\cos\theta)e \otimes e + \sin\theta [e]_x, \tag{5.6}$$

where $\theta \in [0, 2\pi)$ and $e := (e_1, e_2, e_3) \in S^2$ denote the Euler axis of R, respectively, and $[e]_x$ is the crossed product matrix of e. They are given by the formulae:

$$\theta = \arccos\left(\frac{R_{1,1}+R_{2,2}+R_{3,3}-1}{2}\right), \tag{5.7}$$

$$(e_1, e_2, e_3) := \left(\frac{R_{3,2}-R_{2,3}}{2\sin\theta}, \quad \frac{R_{1,3}-R_{3,1}}{2\sin\theta}, \quad \frac{R_{2,1}-R_{1,3}}{2\sin\theta}\right), \tag{5.8}$$

and

$$[e]_x = \begin{pmatrix} 0 & -e_3 & e_2 \\ e_3 & 0 & -e_1 \\ -e_2 & e_1 & 0 \end{pmatrix}.$$

Since the Euler axis e is in S^2, e is represented as the spherical Euler angles $(\phi, \psi) \in [0, \pi) \times [0, 2\pi)$. Therefore, R is represented as three parameters $(\theta, \psi, \phi) \in [0, 2\pi) \times [0, \pi) \times [0, 2\pi)$.

5.3.3. Setting

We use the following initial data u with the Euler angles $\theta, \phi, \psi : (0,1) \times (0,1) \to \mathbb{R}$:

$$\theta := \sum_{i,j=0}^{2} \boldsymbol{\theta}_{i,j} \mathbf{1}_{I_i \times J_j}, \quad \phi := \sum_{i,j=0}^{2} \boldsymbol{\phi}_{i,j} \mathbf{1}_{I_i \times J_j}, \quad \psi := \sum_{i,j=0}^{2} \boldsymbol{\psi}_{i,j} \mathbf{1}_{I_i \times J_j}, \tag{5.9}$$

where

$$\boldsymbol{\theta} = \begin{pmatrix} 0.35\pi & 0.2\pi & 0.55\pi \\ 0.81\pi & 0.64\pi & 0.4\pi \\ 0.1\pi & 0.7\pi & 0.3\pi \end{pmatrix}, \quad \boldsymbol{\phi} = \begin{pmatrix} 0.4\pi & 0.5\pi & 0.7\pi \\ 0.5\pi & 0.3\pi & 0.4\pi \\ 0.6\pi & 0.3\pi & 0.4\pi \end{pmatrix},$$
$$\boldsymbol{\psi} = \begin{pmatrix} 0.2\pi & 0.25\pi & 0.3\pi \\ 0.25\pi & 0.225\pi & 0.2\pi \\ 0.3\pi & 0.2\pi & 0.35\pi \end{pmatrix},$$

and

$$I_0 = \left(0, \frac{2}{5}\right), \quad I_1 = \left(\frac{2}{5}, \frac{3}{5}\right), \quad I_2 = \left(\frac{3}{5}, 1\right),$$
$$J_0 = \left(0, \frac{1}{5}\right), \quad J_1 = \left(\frac{1}{5}, \frac{4}{5}\right), \quad J_2 = \left(\frac{4}{5}, 1\right).$$

Figures 3, 4, 5 and 6 depict the results of numerical experiments under the above setting at time $t = 0.0, 0.05, 0.1, 0.15$, $t = 0.2, 0.25, 0.35, 0.45$, $t = 0.5, 0.55, 0.6, 0.65$, and $t = 0.7, 0.8, 0.85, 1.0$, respectively. Although there does not exist any benchmark test for $SO(3)$-valued TV flow, we can see that our proposed numerical scheme works well since the facet-preserving phenomenon is observed and the numerical solution finally reaches the constant solution.

A. The constant C_M

In this section, we explain a bound of the constant C_M which appears in (2.2). We recall several notations developed in the computational geometry. A point $x \in \mathbb{R}^\ell$ is said to have the unique nearest point if there exists a unique point $p(x) \in M$ such that $p(x) \in \arg\min_{p \in M} \|x - p\|_{\mathbb{R}^\ell}$. Let $S_0(M)$ denote the set of all points in $\mathbb{R}^\ell$ which *do not* have the unique nearest point. The closure $S(M)$ of $S_0(M)$ is called the medial axis of M. The local feature size $\mathrm{LFS}(M)$ of M is the quantity defined by

$$\mathrm{LFS}(M) := \inf_{p \in M} \inf_{q \in S_0(M)} \|p - q\|_{\mathbb{R}^\ell} .$$

Now, we assume that M is a compact. Then, $\mathrm{LFS}(M)$ is positive since M is C^2 so that M has positive reach ([12]). We use the quantity $\mathrm{LFS}(M)$ to obtain that

$$\|p - q\|_{\mathbb{R}^\ell} \leq \mathrm{Dist}_M(p, q) \leq 2 \max\left\{1, \frac{\mathrm{Diam}(M)}{\mathrm{LFS}(M)}\right\} \|p - q\|_{\mathbb{R}^\ell} \tag{A.1}$$

for each point p and q in M. Here, $\mathrm{Dist}_M(p, q)$ denotes the geodesic distance between p and q. On the other hand, assuming that M is path-connected, we have

$$\left\|\pi_p^\perp(p - q)\right\|_{\mathbb{R}^\ell} \leq \frac{1}{2} \mathrm{Curv}(M) \ \mathrm{Dist}_M(p, q)^2 \tag{A.2}$$

for all $p, q \in M$. Therefore, if M is a path-connected and a compact submanifold of $\mathbb{R}^\ell$, then we plug the inequalities (A.2) and (A.1) to obtain

$$\left\|\pi_p^\perp(p - q)\right\|_{\mathbb{R}^\ell} \leq 2 \ \mathrm{Curv}(M) \ \max\left\{1, \frac{\mathrm{Diam}(M)}{\mathrm{LFS}(M)}\right\}^2 \|p - q\|_{\mathbb{R}^\ell}^2 \tag{A.3}$$

for all $p, q \in M$. Hence, we have

$$C_M \leq 2 \ \mathrm{Curv}(M) \ \max\left\{1, \frac{\mathrm{Diam}(M)}{\mathrm{LFS}(M)}\right\}^2 . \tag{A.4}$$

Finally, we remark that the proofs of (A.1) and (A.2) are found in [32].

References

[1] P.-A. Absil, R. Mahony and R. Sepulchre, Optimization algorithms on matrix manifolds, xvi+224 pp., *Princeton University Press, Princeton, NJ* (2008)

[2] L. Ambrosio, N. Gigli and G. Savare, Gradient flows in metric spaces and in the space of probability measures, Lectures in Mathematics ETH Zürich, viii+333 pp., *Birkhäuser Verlag, Basel* (2005)

[3] J.W. Barrett, X. Feng and A. Prohl, On p-harmonic map heat flows for $1 \leq p < \infty$ and their finite element approximations, *SIAM J. Math. Anal.* **40**, 1471–1498 (2008)

[4] P.J. Basser, J. Mattiello and D. LeBihan, MR diffusion tensor spectroscopy and imaging, *Biophysics J.* **66**, 259–267 (1994)

[5] A. Di Castroa and L. Giacomelli, The 1-harmonic flow with values into a smooth planar curve, *Nonlinear Anal.* **143**, 174–192 (2016)

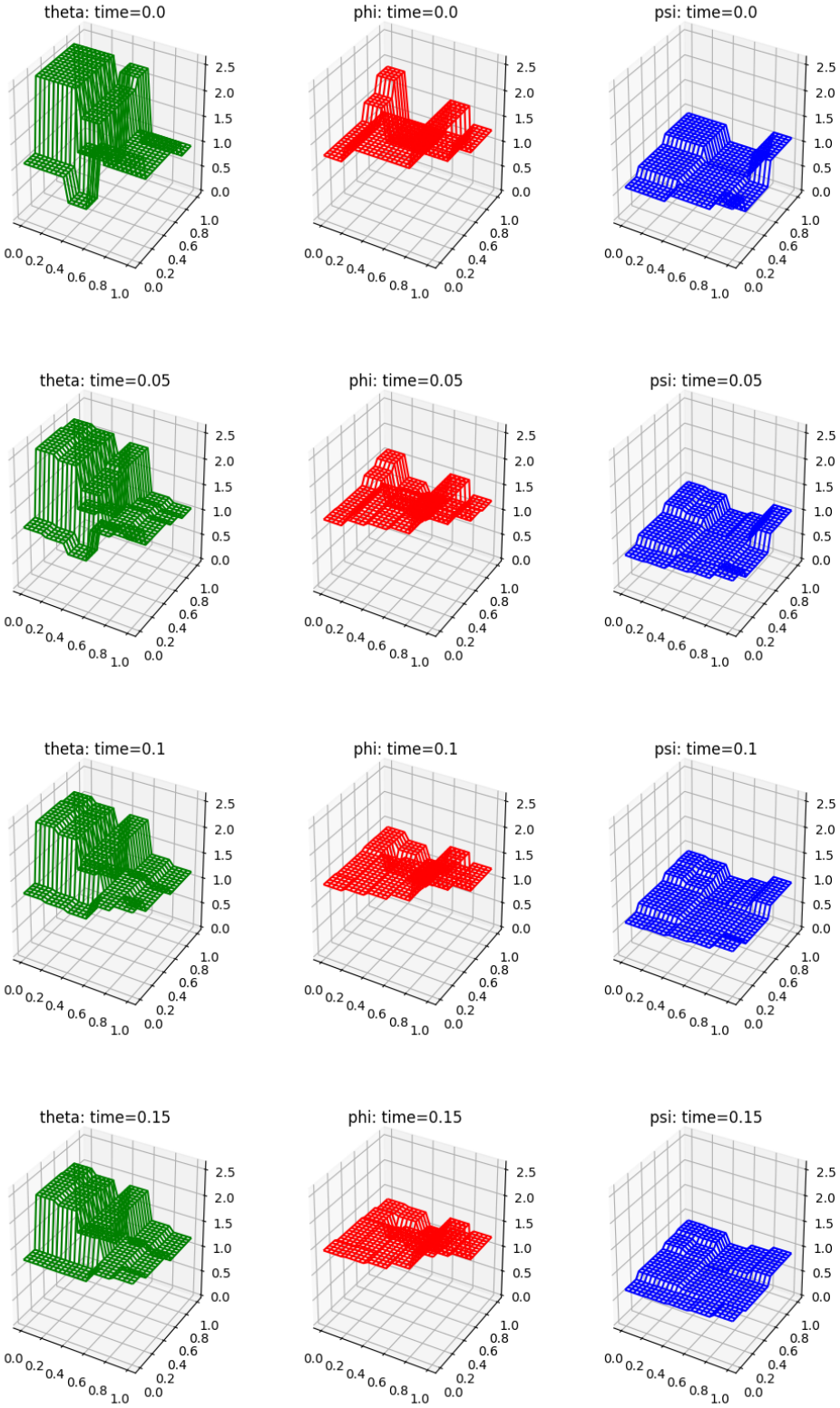

Figure 3: Numerical simulation of $SO(3)$-valued TV flow at $t = 0.0, 0.05, 0.1, 0.15$.

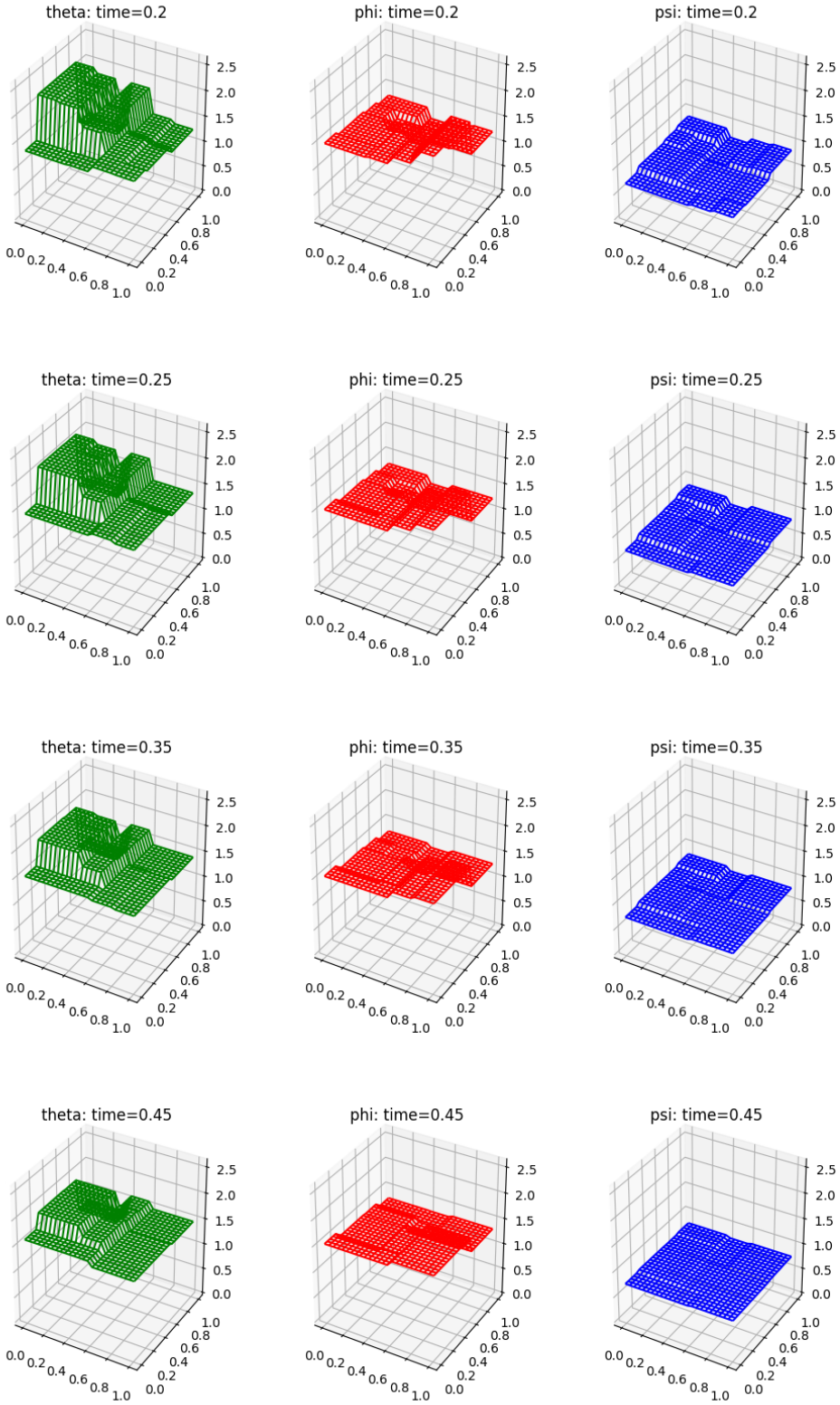

Figure 4: Numerical simulation of $SO(3)$-valued TV flow at $t = 0.2, 0.25, 0.35, 0.45$.

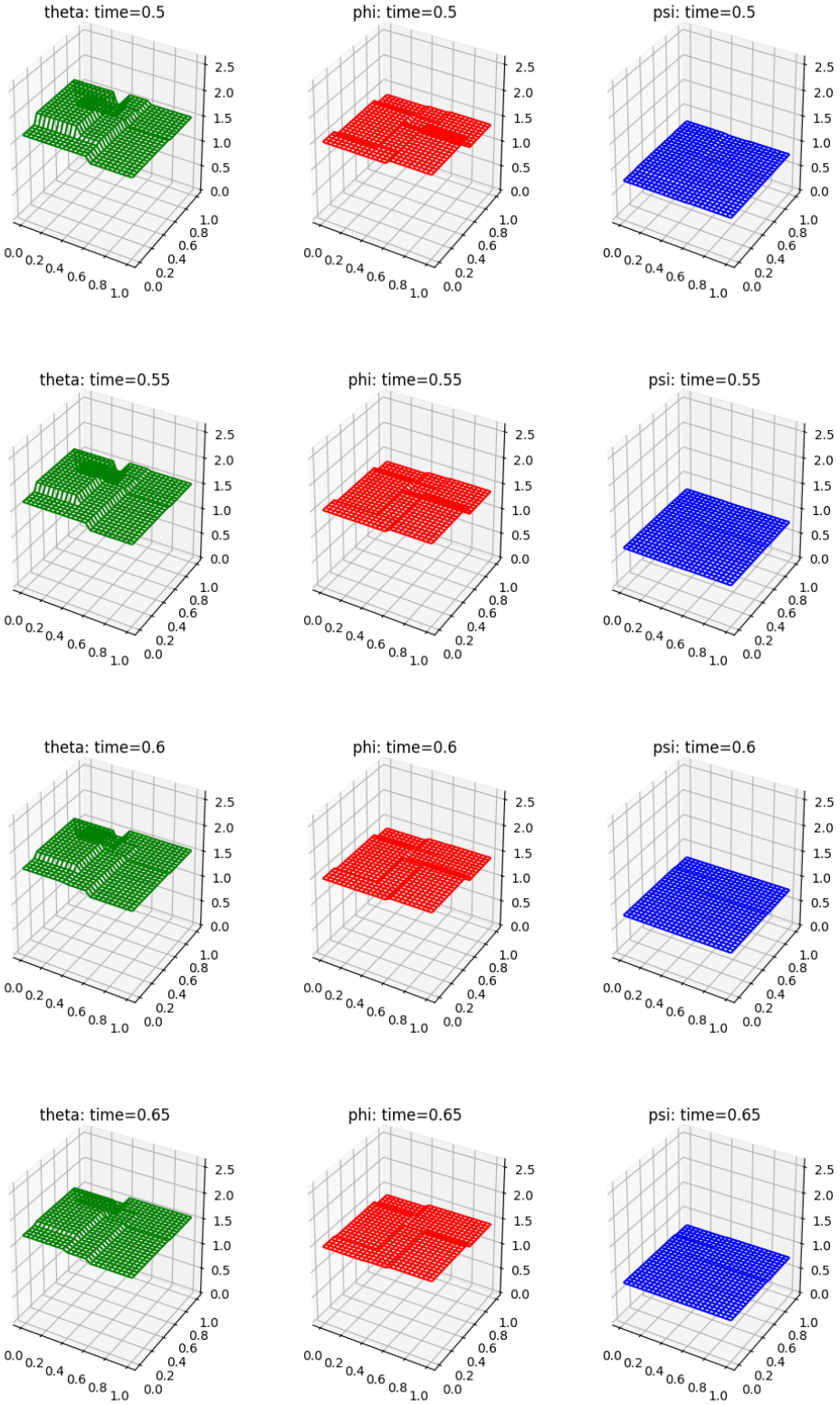

Figure 5: Numerical simulation of $SO(3)$-valued TV flow at $t = 0.5, 0.55, 0.6, 65$.

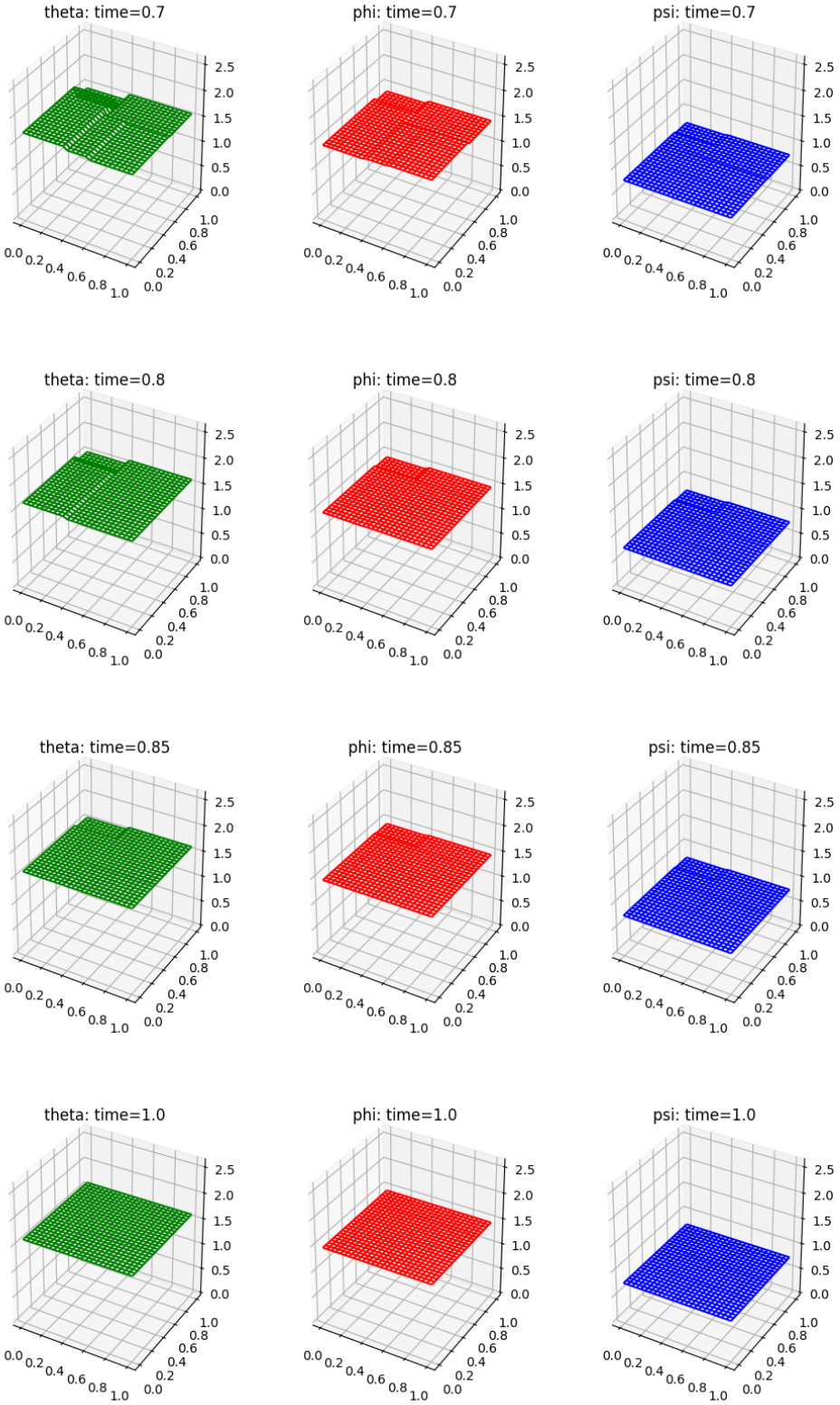

Figure 6: Numerical simulation of $SO(3)$-valued TV flow at $t = 0.7, 0.8, 0.85, 1.0$.

[6] C. Chefd'hotel, D. Tschumperlé, R. Deriche and O. Faugeras, Constrained flows of matrix-valued functions: application to diffusion tensor regularization, *Computer Vision-ECCV 2002*, 251–265 (2002).

[7] C. Chefd'hotel, D. Tschumperlé, R. Deriche and O. Faugeras, Regularizing flows for constrained matrix-valued images, *J. Math. Imaging Vision* **20**, 147–162 (2004).

[8] A. Kovnatsky, K. Glashoff and M.M. Bronstein, MADMM: A generic algorithm for non-smooth optimization on manifolds, *Computer Vision-ECCV 2016*, 680–696 (2016).

[9] O. Christiansen, T.-M. Lee, J. Lie, U. Sinha and T.F. Chan, Total variation regularization of matrix-valued images, *International journal of biomedical imaging* **2007**, 11 pp. (2007)

[10] M.G. Crandall and T.M. Liggett, Generation of semi-groups of nonlinear transformations on general banach spaces, *Amer. J. Math.* **93**, 265–298 (1971)

[11] X. Feng and M. Yoon, Finite element approximation of the gradient flow for a class of linear growth energies with applications to color image denoising, *Int. J. Numer. Anal. Model.* **6**, 389–401 (2009)

[12] R.L. Foote, Regularity of the distance function, *Proc. Amer. Math. Soc.* **92**, 1187–1220 (1984)

[13] L. Giacomelli, J.M. Mazón and S. Moll, The 1-harmonic flow with values into $\mathbb{S}^1$, *SIAM J. Math. Anal.* **45**, 1723–1740 (2013)

[14] L. Giacomelli, J.M. Mazón and S. Moll, The 1-harmonic flow with values in a hyperoctant of the N-sphere, *Anal. PDE* **7**, 627–671 (2014)

[15] L. Giacomelli and M. Łasica and S. Moll, Regular 1-harmonic flow, *arXiv:1711.07460*, 24 pp. (2017)

[16] Y. Giga and R. Kobayashi, On constrained equations with singular diffusivity, *Methods Appl. Anal.* **10**, 253–278 (2003)

[17] Y. Giga and H. Kuroda, On breakdown of solutions of a constrained gradient system of total variation, *Bol. Soc. Parana. Mat.* **22**, 9–20 (2004)

[18] Y. Giga, H. Kuroda and N. Yamazaki, An existence result for a discretized constrained gradient system of total variation flow in color image processing, *Interdiscip. Inform. Sci.* **11**, 199–204 (2005)

[19] Y. Giga, H. Kuroda and N. Yamazaki, Global solvability of constrained singular diffusion equation associated with essential variation, *Internat. Ser. Numer. Math.* **154**, 209–218 (2006)

[20] Y. Giga and H. Kuroda, A counterexample to finite time stopping property for one-harmonic map flow, *Commun. Pure Appl. Anal.* **14**, 1–5 (2015)

[21] T. Goldstein and S. Osher, The split Bregman method for L^1-regularized problems, *SIAM J. Imaging Sci.* **2**, 323–343 (2009)

[22] R. Kobayashi and J.A. Warren, Modeling the formation and dynamics of polycrystals in 3D, *Phys. A* **356**, 127–132 (2005)

[23] R. Kobayashi and J.A. Warren and W.C. Carter, A continuum model of grain boundaries, *Phys. D* **140**, 141–150 (2000)

[24] R. Lai and S.J. Osher, A splitting method for orthogonality constrained problems, *J. Sci. Comput.* **58**, 431–449 (2014)

[25] G. Li and T.K. Pong, Global convergence of splitting methods for nonconvex composite optimization, *SIAM J. Optim.* **25**, 2434–2460 (2015)

[26] A. Oberman and S. Osher and R. Takei and R. Tsai, Numerical methods for anisotropic mean curvature flow based on a discrete time variational formulation, *Commun. Math. Sci.* **9**, 637–662 (2011)

[27] R. Dal Passo and L. Giacomelli and S. Moll, Rotationally symmetric 1-harmonic maps from D^2 to S^2, *Calc. Var. Partial Differential Equations* **32**, 533–554 (2010)

[28] X. Pennec and P. Fillard and N. Ayache, A Riemannian framework for tensor computing, *International Journal of Computer Vision* **66**, 41–66 (2006)

[29] N. Požár, On the self-similar solutions of the crystalline mean curvature flow in three dimensions, *arXiv:1806.02482*, 28 pp. (2018)

[30] J. Rulla, Error analysis for implicit approximations to solutions to Cauchy problems, *SIAM J. Numer. Anal.* **33**, 68–87 (1996)

[31] S. Setzer, *Splitting methods in image processing*, *Ph.D thesis, Universitat Mannheim*, 174 pp. (2009)

[32] K. Taguchi, On discrete one-harmonic map flows with values into an embedded manifold on a multi-dimensional domain, *Adv. Math. Sci. Appl.* **27**, 81–113 (2018)

[33] B. Tang and G. Sapiro and V. Caselles, Color image enhancement via chromaticity diffusion, *IEEE Transactions on Image Processing* **10**, 701–707 (2001)

[34] L.A. Vese and S.J. Osher, Numerical methods for p-harmonic flows and applications to image processing, *SIAM J. Numer. Anal.* **40**, 2085–2104 (2009)

[35] A. Weinmann and L. Demaret and M. Storath, Total variation regularization for manifold-valued data, *SIAM J. Imaging Sci.* **7**, 2226–2257 (2014)

[36] Y. Wang and W. Yin and J. Zeng, Global convergence of ADMM in nonconvex nonsmooth optimization, *J. Sci. Comput.*, 35 pp. (2018)

[37] J. Zhang, S. Ma and S. Zhang, Primal-Dual optimization algorithms over Riemannian manifolds: an iteration complexity analysis, *arXiv:1710.02236*, 44 pp. (2017)